STRUCTURE AND FUNCTION OF PROTEINS INVOLVED IN REGULATED SECRETION: COMPLEXIN AND SYNAPTOTAGMINS

APPROVED BY SUPERVISORY COMMITTEE

_____

_____

_____

_____

DEDICATION

This work is dedicated to my family for their unwavering love and support. I would also like to thank the members of my committee, friends, and colleagues for their assistance in matters both scientific and personal. I would also like to especially acknowledge my mentor, José Rizo-Rey for his knowledge, skills, and patience throughout my graduate career at UT Southwestern Medical Center.

STRUCTURE AND FUNCTION OF PROTEINS INVOLVED IN REGULATED SECRETION: COMPLEXIN AND SYNAPTOTAGMINS

by

TIMOTHY KELLOGG CRAIG

DISSERTATION

Presented to the Faculty of the Graduate School of Biomedical Sciences

The University of Texas Southwestern Medical Center at Dallas

In Partial Fulfillment of the Requirements

For the Degree of

DOCTOR OF PHILOSOPHY

The University of Texas Southwestern Medical Center at Dallas

Dallas, Texas

September, 2009

STRUCTURE AND FUNCTION OF PROTEINS INVOLVED IN REGULATED SECRETION: COMPLEXIN AND SYNAPTOTAGMINS

TIMOTHY KELLOGG CRAIG, Ph.D

The University of Texas Southwestern Medical Center at Dallas, 2009

Josep Rizo-Rey,Ph.D

The release of neurotransmitter from neurons is a tightly regulated process. There are a number of proteins required for membrane fusion to occur, and then there are regulatory proteins that allow membrane fusion to proceed at incredible speed with the precise timing necessary for complex functions such as sight, motor control, and conscious thought. This study will explore the role of three such regulators through biophysical and structural methods.

There are a number of proteins that are essential for membrane fusion. The SNARE proteins are the plasma membrane protein Syntaxin, the vesicle membrane protein Synaptobrevin, and the plasma membrane associated protein SNAP25. These proteins form a tight complex called the SNARE complex that is required for

neurotransmitter release. This complex bridges the vesicle and plasma membranes, bringing them into close proximity. Formation of this complex is thus an important point of regulation for the neurotransmitter release process. This SNARE complex serves not only to bridge two membranes, but also to become an anchoring point for a number of regulators of neurotransmitter release such as Complexin, and Synaptotagmin as well as other required proteins such as Munc13 and Munc18.

Complexin is a small soluble protein that binds to the SNARE complex with high affinity and regulates the formation of the SNARE complex. Synaptotagmin is the calcium sensor for fast release of neurotransmitter. Here I present data showing that the N-terminus of Complexin is involved in a critical interaction with the C-terminus of the SNARE complex that is responsible for the excitatory effect of complexin in neurotransmitter release.

Synaptotagmins work with Complexins to trigger rapid membrane fusion in response to calcium influx. Synaptotagmin VII is an important protein for the release of glucagon from islets of langerhans. The C2B domain of this protein is nearly 50% identical to the C2B domain of SytI, but when the C2B domains of SytVII and SytI are switched, the protein does not function correctly. In this study the structure of SytVII was determined by x-ray crystallography to 1.44Å resolution in order to determine if the C2B domain of SytVII is structurally different from other C2B domains. Additionally I crystallized and solved the structure of the C2A domain of Synaptotagmin IX in an effort to compare it to the C2 domains of the other members of the synaptotagmin family. This analysis resulted in the surprising conclusion that a high degree of structural similarity does not necessarily relate to interoperability of the domains.

TABLE OF CONTENTS

PRIOR PUBLICATIONS

Xue M, Ma C, Craig TK, Rosenmund C, Rizo J. The Janus-faced nature of the C(2)B domain is fundamental for synaptotagmin-1 function. Nat Struct Mol Biol. 2008 Nov;15(11):1160-8. Epub 2008 Oct 26.

LIST OF FIGURES

LIST OF TABLES

LIST OF ABBREVIATIONS

1D, 2D, 3D	**One dimensional, 2 Dimensional, etc**
C.elegans	***Caenorhabditis elegans***
SDS-PAGE	**Sodium Dodecyl Sulfate- polyacrylamid gel electrophoresis**
CMC	**Critical Micellar Concentration**
CPXS	**Rat complexin 1 (residues 26-83)**
CpxI	**Rat complexin 1**
CpxII	**Rat complexin II**
CpxIII	**Rat complexin III**
CpxIV	**Rat complexin IV**
CSA	**Chemical shift anisotropy**
DD	**Dipole-Dipole interaction**
DLS	**Dynamic light scattering**
DOPS	**1,2-dioleoyl phosphatidylserine**
DTT	**Dithiothreitol**
E.coli	***Eschericheria coli***
EDTA	**Ethylene diamine tetraacedic acid**
EGTA	**Ethylene glycol-bis (β-aminoethyl ether)-tetraacetic acid**
FPLC	**Fast performance liquid chromatography**
FRET	**Förster resonance energy transfer**
GST	**Glutathione S-Transferase**
HEPES	**N-(2-hydroxyethyl) piperizine-N'2-ethanesulphonic acid**
HSQC	**Heteronuclear single quantum coherence spectroscopy**
	Isopropyl β-D-thiogalactopyranoside
K_D	**Dissociation constant**
KDa	**Kilodalton**
LB	**Luria Broth**
LMV	**Large multilamellar vesicles**
LUV	**Large unilamellar vesicles**
Ni-NTA	**Nickel-nitrilotriacetic acid**
NMR	**Nuclear Magnetic Resonance**
NSF	**N-ethylmaleimide-sensitive factor**
SN1	**N-terminal SNARE motif of rat SNAP25**
SN3	**C-terminal SNARE motif of rat SNAP25**

OD	**Optical density**
OG	**Octyl-β-D-glucopyranoside**
PBS	**Phosphate buffered saline**
PC	**phosphatidylcholine**
PCR	**Polymerase chain reaction**
PE	**phosphatidylethanolamine**
POPC	**1-palitoyl, 2-oleoyl phosphatidylcholine**
Ppm	**Part per million**
PS	**phosphatydlserine**
Reff	**Effective detergent to lipid ratio**
rmsd	**Root mean square deviation**
Rsat	**Effective ratio at the onset of solubilization of liposomes**
rsol	**Effective ratio at the total solubilization of liposomes**
SNAP-25	**Rat synaptosome associated protein-25KDa**
SNARE	**SNAP receptor**
Syb2	**Rat synaptobrevin 2**
Syx	**Rat syntaxin 1A**
SyxS	**Rat syntaxin 1A (191-253)**
TRIS	**Tris (hydroxymethyl) aminomethane**
Trosy	**Transverse relaxation optimized spectroscopy**
t-SNARE	**Target membrane SNARE**
UV	**Ultraviolet**
VAMP	**Vesicle assosciated membrane protein**
V-SNARE	**Vesicle SNARE**

CHAPTER ONE
Introduction

1.1 The Synaptic Vesicle Cycle

The brain is composed of a network of about 10^{11} neurons, each connecting to thousands of other neurons. This incredibly complex network of neural cells is the basis for cognition, motor control, learning and memory, and even emotion. In order to effect these functions, individual brain cells, or neurons, must be able to transmit information to other neurons. This is accomplished through both electrical and chemical means using a variety of methods. This thesis will focus mainly on chemical neurotransmission, in which a chemical neurotransmitter, such as dopamine, serotonin, or glutamate, is physically released onto another cell at a specialized part of the cell membrane called the active zone.

Neurons are comprised of three main anatomical parts, which are depicted in **Figure 1**. The cell body contains the nucleus and is the location of protein synthesis for nearly all protein in the cell. The characteristically long axon is the major distance spanning component of the cell. This part of the cell has evolved mechanisms such as the myelin sheath to improve electrical conduction across large distances. The dendrites are highly branched extensions of the cell body and which typically receive input from the axons of other neurons. The site of this

physical contact and the site of neurotransmission of information is called the synapse.

Electron microscopy studies of synapses have shown these synapses to be highly enriched with protein(Gray 1959), indicating that a highly coordinated protein machinery enables the synaptic vesicle cycle and membrane fusion. The synaptic vesicle cycle is the process by which new synaptic vesicles are created, trafficked to the plasma membrane, primed for neurotransmitter release, fused with the plasma membrane, and then recycled. This process is depicted in **Figure 2**(Sudhof 1995). Synaptic vesicles bud off from the early endosome and are filled with neurotransmitter by specialized membrane transporter proteins. These proteins are able to transport the sometimes highly charged substrates across a membrane using ATP as an energy source for overcoming the free energy barrier created by partitioning a high concentration of neurotransmitter into a synaptic vesicle. After the vesicles have been filled, they are trafficked by vesicle transport proteins to a specialized area of the plasma membrane on the presynaptic side of the synapse called the active zone. Upon docking, a protein complex partially forms to bring the vesicle and plasma membranes into close proximity. After this, the "priming" step occurs. This process is thought to involve a number of proteins as well as ATP. The result of the priming process is a vesicle and plasma membrane that are being held in a metastable state that can fuse rapidly upon influx of calcium.

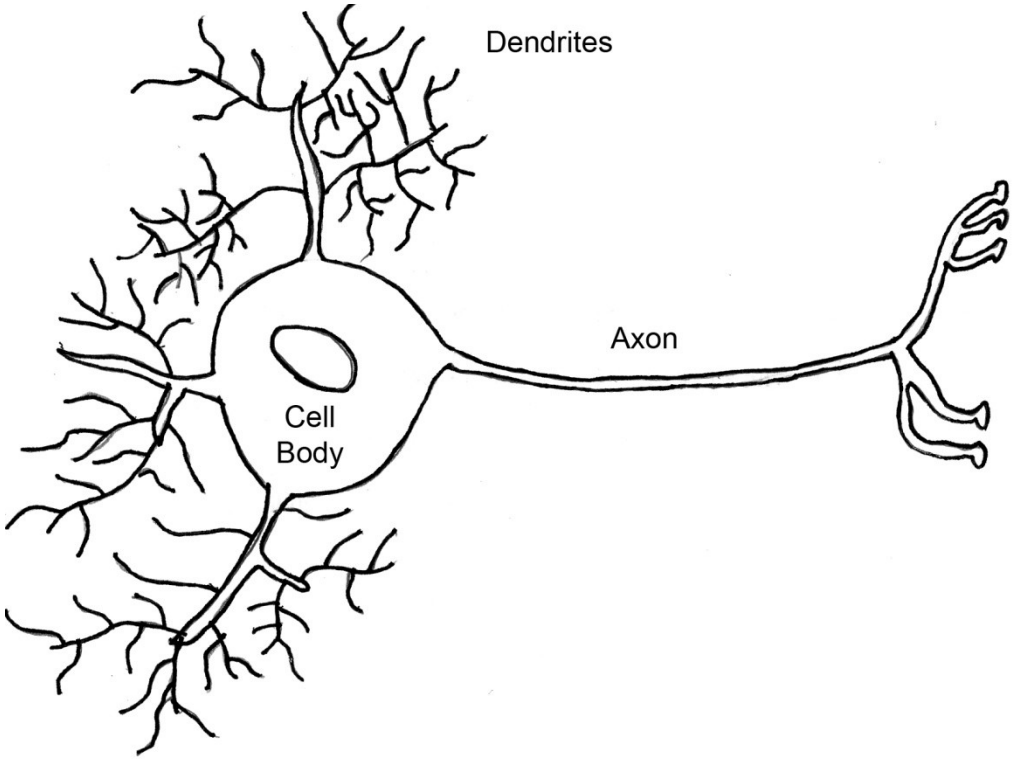

Figure 1. Anatomy of a typical neuron. There are three specialized anatomical regions of the cell: the axon, dendrites, and the soma. Figure by Craig TK

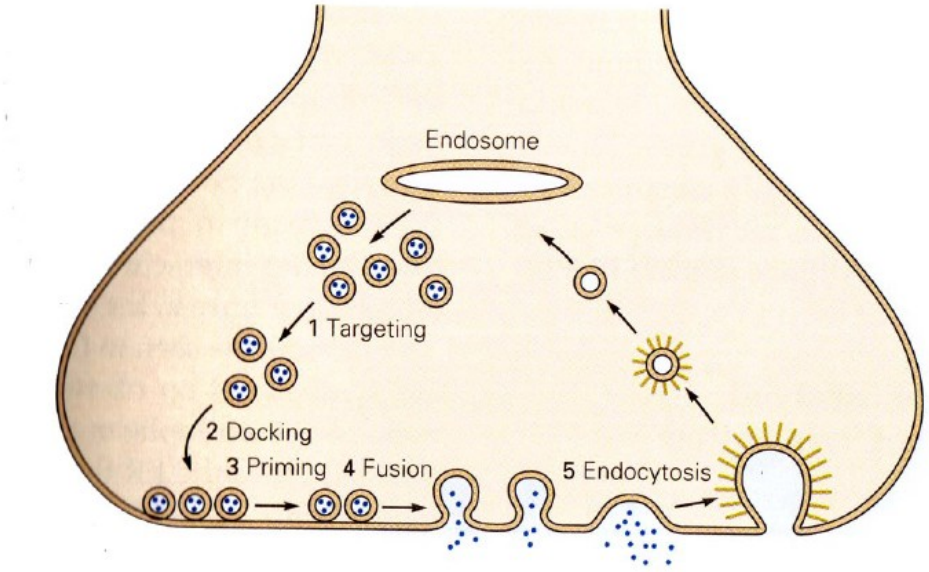
Endosome
1 Targeting
2 Docking
3 Priming
4 Fusion
5 Endocytosis

Figure 2 Diagram of the synaptic vesicle cycle (From (Sudhof 1995)). Vesicles bud off from the endosome, where they are filled with neurotransmitter and trafficked to the active zone, where they undergo a docking and priming process that prepares them for fusion. Upon calcium influx, the vesicles fuse with the membrane and release neurotransmitters into the synaptic cleft. After exocytosis, sections of the membrane are endocytosed and brought back to the endosome where the cycle begins again. Fusion occurs within 0.5 msec(Sabatini and Regehr 1999) of calcium influx from voltage gated calcium channels that are opened by action potentials. At this point, vesicles can either fuse completely with the plasma membrane, and then be recycled in a clatherin-dependent manner. Alternatively, they can engage in so-called "kiss and run" neurotransmitter release(Fesce, Grohovaz et al. 1994), where the fusion pore does not rapidly expand, but rather flickers open and then closes off. In either case, the vesicles are trafficked back to be charged with neurotransmitters and fused again. For this project, I have studied the function of proteins in the docking and priming steps of membrane fusion.

1.2 Proteins Involved in Membrane Fusion

The machinery of membrane fusion contains a number of proteins that are essential for fusion (Sudhof 1995; Augustine, Burns et al. 1996; Lin and Scheller 1997; Jahn and Sudhof 1999). These proteins include the SNAREs, SNAPs, NSF, Munc18-1, and Rab3. These proteins are conserved in nearly all species from yeast to human (Bennett and Scheller 1993; Ferro-Novick and Jahn 1994), suggesting an evolutionarily conserved mechanism for membrane fusion. Proteins such as synaptotagmin 1, complexins, and Munc13-1 are required for synaptic transmission, but not other kinds of membrane fusion events(Sollner 2003). These other types of regulated membrane fusion events are important, but do not require the speed of the full neurotransmitter release machinery.

1.3 Individual SNARE Proteins and the SNARE Complex

Individual SNARE proteins contain one or more heptad repeats. These heptad repeats allow SNARE proteins to form a helix bundles. The SNARE complex is extremely stable and thought to serve as both a force generating entity for inducing membrane proximity and as a molecular scaffold for other proteins involved in membrane fusion. The three SNARE proteins that form the neuronal SNARE complex are syntaxin, SNAP25, and synaptobrevin. These proteins are depicted in **Figure 3** (See below).

Syntaxin is a plasma membrane protein with a single transmembrane helix as well as a 3 helix bundle H_{abc} domain. This 36 kDa protein can adopt an open and closed conformation, which exist in equilibrium. The 4 helix bundled closed conformation binds with high affinity to Munc18. The binding site on Syntaxin for Munc18 is the four helix bundle and an N-terminal tail at the start of syntaxin(Misura, Scheller et al. 2000). These two binding sites are important not only for sequestering the SNARE motif of syntaxin to regulate SNARE complex formation, but may also play a role in promoting membrane fusion by acting as a wedge between the vesicle and plasma membranes by virtue of its relative bulk(Dulubova, Khvotchev et al. 2007). This model of Munc18-SNARE interaction would also prevent diffusion of the SNARE complex into the space between the vesicle and plasma membrane. Syntaxin itself is reported to interact with calcium channels (O'connor, Shamotienko et al. 1993) and other important proteins as a part of the SNARE complex(Rizo and Sudhof 2002).

SNAP25 is a membrane associated protein that contributes 2 SNARE motifs to the SNARE complex. This protein consists of an N-terminal SNARE motif known as SN1, a flexible linker region, and a C-terminal SNARE motif called SN3(Chapman, An et al. 1994). The two SNARE motifs of this protein have posed numerous problems for in vitro studies. First is that oligomerization of SNARE complexes is possible by virtue of the flexible region of SNAP25. The second problem is that the separately expressed SN1 protein can form a 2:2

tetramer with syntaxin, which is a kinetically trapped state that cannot form the true SNARE complex. Finally, the four native cysteines of SNAP25 are palmitolyated in vertebrates(Hess, Slater et al. 1992). This post-translational modification could have important implications for the orientation of the protein-protein complexes required for fast neurotransmitter release. Unfortunately, these cysteines are generally ignored or mutated to serines or avoided altogether by using only the SNARE motif fragments for experiments in the literature.

Synaptobrevin, also known as VAMP2, is a vesicle associated membrane protein, and the third and final component of the SNARE complex. Historically, inhibition of neurotransmitter release by specific cleavage of synaptobrevin by clostridial neurotoxins was the first indication that SNARE proteins were involved in neurotransmitter release (Link, Edelmann et al. 1992; Schiavo, Rossetto et al. 1992; Blasi, Chapman et al. 1993; Blasi, Chapman et al. 1993). Synaptobrevin is a relatively simple part of the fusion machinery. Once synaptobrevin begins to bind to the complex formed by the SNAP25 and Syntaxin SNARE motifs, called the t-SNARE complex, the 3 protein complex zippers and forms coiled-coil helices, starting from the N-terminal side of the SNARE motif, unless it is blocked by an interaction with another protein.

This SNARE complex serves as a protein scaffold and as a source of energy for overcoming the high energy barrier of membrane fusion(Rizo and Sudhof 2002). The SNARE complex was first discovered by Sollner et

al(Sollner, Bennett et al. 1993) who showed that the SNARE complex components could form complexes *in vitro* in the absence of other neuronal proteins. This highly stable SNARE complex was shown to be dissociated by the ATPase activity of NSF (Hayashi, Yamasaki et al. 1995). Cleavage of the SNAREs by clostridial neurotoxins showed that the SNARE complex acts downstream of docking (Link, Mcmahon et al. 1993), supporting the idea that the SNARE complex provides force for fusing membranes. The crystal structure of the SNARE complex was solved in 1988 by Sutton et al and revealed that the SNARE complex was composed of 4 parallel coiled coils (Sutton, Fasshauer et al. 1998). A cartoon diagram of the SNARE complex as it would look in a membrane environment is shown in **Figure 4**.

1.4 Complexins

As the importance of the SNARE complex became clear, SNARE binding proteins and their effect on the state of the complex and on membrane fusion began to be investigated. Complexin was identified by GST pull-down as a complex-interacting protein that colocalizes with SNAP25 and Syntaxin(Mcmahon, Missler et al. 1995). Further studies revealed the very tight binding of CpxI with the SNARE complex (Pabst, Margittai et al. 2002; Bowen, Weninger et al. 2005; Liu, Guo et al. 2006; Li, Augustine et al. 2007). Using NMR spectroscopy, a SNARE binding helix was identified in this protein

(residues 26-83) only in the presence of soluble SNARE complex (Pabst, Hazzard et al. 2000). In its apo form, complexin is unstructured (Pabst, Hazzard et al. 2000). This binding data led to the eventual crystallization and structure of the SNARE/Complexin complex, which was solved in our laboratory (Chen, Tomchick et al. 2002). The structure showed an anti-parallel binding mode of complexin, with the N-terminus of the C and N-terminally shortened CpxS (residues 26-83) construct binding to the C-terminus of the SNARE complex. Further hydrogen/deuterium exchange experiments showed that CpxS binding stabilized

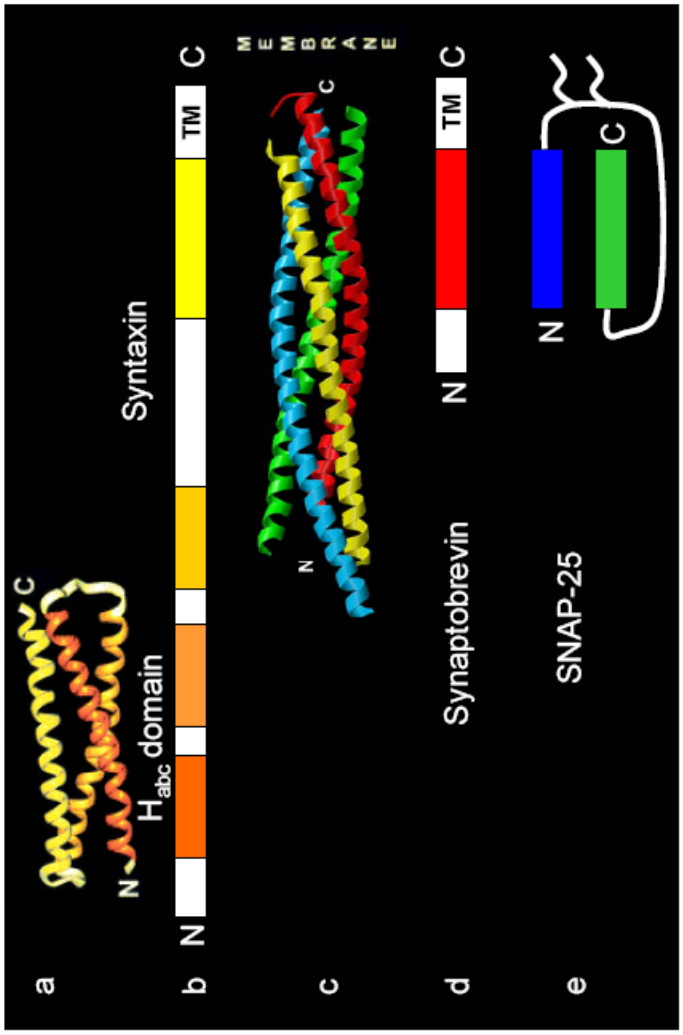
a
b
c
d
e
N
C
Syntaxin
H_{abc} domain
TM
MEMBRANE
Synaptobrevin
SNAP-25

Figure 3 Structure of the SNARE complex and its components. (A), The structure of the Syntaxin Habc domain(Fernandez, Ubach et al. 1998) is shown next to a domain diagram (B) of its primary structure. TM stands for transmembrane domain. A similar diagram is shown for Synaptobrevin (D) and SNAP25 (E). The structure of the SNARE complex(Sutton, Fasshauer et al. 1998) is shown in part C with each of the 4 SNARE motifs: Syntaxin (**Yellow**), Synaptobrevin (**Red**), and the N (**Blue**) and C (**Green**)-terminal SNARE motifs of SNAP25. The four SNARE motifs bind in a parallel fashion with the C-terminal region of the complex being closest to the membrane**.**

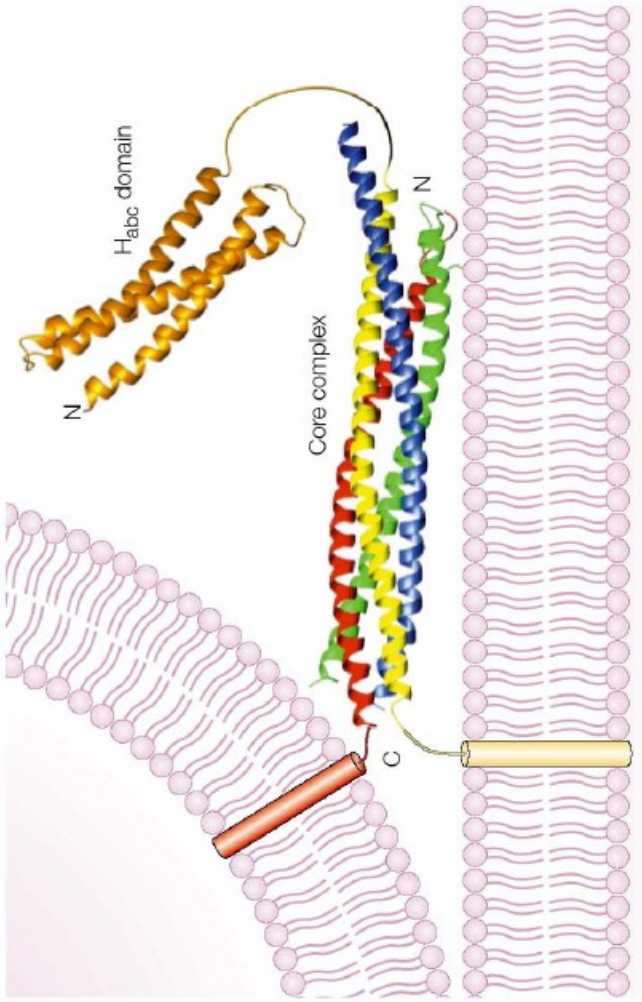
H_{abc} domain
N
Core complex
N
C

Figure 4 A model of the SNARE complex in the context of the membranes. The parallel binding of the SNARE motifs causes the vesicle and plasma membranes to come into close proximity. The diagram uses the crystal structure of the SNARE complex and the NMR structure of the Syntaxin H_{abc} domain. Each of the SNARE motifs are colored similarly to **Figure 3.** The transmembrane regions are shown as cylinders and flexible linkers are shown as curved lines.

the SNARE complex, which would contribute to an overall effect of promoting membrane fusion. This result was one of many seemingly conflicting reports about the function of complexin in the literature.

Complexin I/II double knockout in mice causes death upon birth due to a dramatic loss of neurotransmitter release.(Reim 2001) However, despite this lethal phenotype, a number of important effects of complexin were determined using electrophysiology on embryonic brain cells. These cells showed a dramatic decrease in the efficiency of Ca^{2+}-dependent neurotransmitter release, while stimulation with 500mM Sucrose gives a normal phenotype.(Reim, Mansour et al. 2001) This suggests that complexin acts at a late stage of neurotransmitter release, and that it acts as a facilitator. In addition, protein levels and expression of Complexins have been shown to be involved in numerous diseases such as Huntington's(Morton and Edwardson 2001; Edwardson, Wang et al. 2003), schizophrenia(Eastwood, Burnet et al. 2000; Sawada, Young et al. 2002), and bipolar disorder(Eastwood and Harrison 2000), further indicating a modulatory role in neurotransmitter release. Further confusion regarding this protein was introduced when it was shown that overexpression or microinjection results in inhibition of neurotransmitter release(Liu, Guo et al. 2007), suggesting that complexin acts as an inhibitor of neurotransmitter release. These seemingly conflicting reports have led to confusion about the function of complexin.

This contradiction was later explained by a number of pieces of information. First, there is a competition between Synaptotagmin and the complexin central α-helix for binding on the SNARE complex (Tang, Maximov et al. 2006). This was shown in a variety of ways, but most clearly by the displacement of fluorescent CpxS from supported bilayers containing reconstituted SNARE complexes in response to Syt and Ca^{2+}. Under this model, CpxS helps to stabilize the SNARE complex and hold the fusion machinery in a metastable state that is released by Syt and Ca^{2+}(Chen 2002). This model ascribed both a positive and negative role of complexin in neurotransmitter release.

In addition, it was first proposed by our collaborators in the Rosenmund lab that the accessory helix of CpxI could take the place of the C-terminus of synaptobrevin on the SNARE complex(Xue, Reim et al. 2007). This would help complexes of the correct stoichiometry to form by taking the binding site of a second Syntaxin or SN1 on the t-SNARE complex, and would also block fusion by preventing the full zippering of synaptobrevin. This model of complexin function was supported by data from Giraudo et al in 2009(Giraudo, Garcia-Diaz et al. 2009). However, a problem arose in 2007 when work from Xue et al(Xue, Reim et al. 2007) showed that the first 26 residues of complexin were required, along with the SNARE binding central α-helix binding, to rescue the CpxI I/II DKO phenotype(Xue, Reim et al. 2007). The problem these results presented is

that much of the previous work, including the microchannel complexin-displacement assay(Tang, Maximov et al. 2006; Dai, Shen et al. 2007; Roggero, De Blas et al. 2007), was performed not using the full length protein, but with the central α-helix binding portion of the protein known as CpxS, which corresponds to residues 26-83. This construct was missing a number of key residues that are responsible for complexin function *in vivo (Xue, Reim et al. 2007)*. Clearly, the elucidation of the functional partners for the N-terminus of CpxI would have important implications

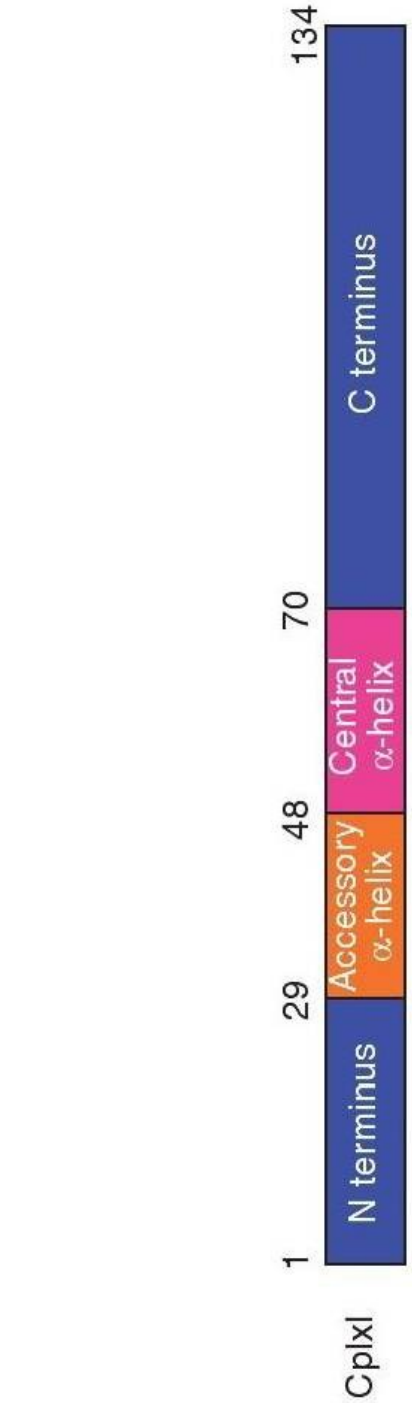
Cplxl
1
29
48
70
134
N terminus
Accessory α-helix
Central α-helix
C terminus

Figure 5 Diagram of the distinct regions of CpxI. Complexin is 134 residues. The first 29 residues are considered to be the N-terminus that is required for CpxI function. Residues 29 to 48 correspond to the inhibitory accessory helix. The central SNARE binding central α-helix consists of residues from 49 to 70. The C-terminus of CpxI corresponds to residues 71-134. Figure from(Xue, Reim et al. 2007)

for neurotransmitter release, and was the main focus of my work. In my results I show that the N-terminus of complexin binds back to SNARE complexes using NMR and fluorescence data.

1.5.1 Synaptotagmins

Synaptotagmins are proteins that regulate membrane fusion events by virtue of their C2 domains. C2 domains are Ca2+/phospholipid binding domains that are similar in structure to the C2 domain of protein kinase C(Fernandez-Chacon 2001). Mutations in SytI that abolish calcium binding have been shown to alter the calcium sensitivity of fast neurotransmitter release while leaving the slow, asynchronous component of release unaltered.(Littleton, Stern et al. 1993; Nonet, Grundahl et al. 1993; Geppert and Sudhof 1998; Fernandez-Chacon 2001) In addition, the calcium affinity of SytI and the calcium sensitivity of neurotransmitter release are very similar(Fernandez-Chacon 2001). These results led to the conclusion that SytI is the calcium sensor for fast neurotransmitter release.

Synaptotagmin I is the major calcium sensor for fast neurotransmitter release(Fernandez-Chacon 2001). The protein is composed of two C2 domains that are attached to the vesicle membrane by a transmembrane domain and a long flexible linker(Perin, Fried et al. 1990) as shown in **Figure 6**. Both domains were named as C2s due to their similarity to the C2 domain of protein kinase C. Both

C2A and C2B domains adopt common β-sandwich architectures (Sutton, Davletov et al. 1995; Shao, Fernandez et al. 1998) . The C2A domain binds 3 Ca^{2+} ions(Fernandez-Chacon, Shin et al. 2002), whereas the C2B binds 2 Ca^{2+} ions and contains HA and HB helices, which currently have no assigned function(Fernandez, Arac et al. 2001). Both C2 domains exhibit low affinity calcium binding in solution, but can bind to Ca^{2+} and phospholipids simultaneously with high affinity(Fernandez-Chacon 2001). The second C2 domain, C2B, was later shown to be able to cluster liposomes in a calcium-dependent manner, revealing that there is a second lipid binding site on the molecule (Arac, Chen et al. 2006). In addition to binding Ca^{2+}/phospholipids, SytI also competes with CpxS for SNARE complex binding (Tang, Maximov et al. 2006; Dai, Shen et al. 2007).

Synaptotagmin I was shown to be the sensor for fast neurotransmitter release in a seminal paper in 2001 by Fernandez-Chacon et al (Fernandez-Chacon 2001). In this report is is demonstrated that a single point mutation (R233Q) at a residue contacting one of the calcium binding loops was able to decrease the Ca^{2+}/phospholipid binding affinity by nearly twofold, while the Ca^{2+} affinity of just the domain in solution actually increased. This point mutation was then expressed in knock-in mice and caused a twofold decrease in the Ca^{2+} affinity of release. This correlation of *in vitro* biophysical data with *in vivo*

electrophysiological data showed that indeed SytI is the calcium sensor for fast neurotransmitter release.

Twelve other Syt isoforms have been discovered, and many of them have different calcium binding affinities and tissue localization from SytI (Sudhof, De Camilli et al. 1993; Sudhof 2002)). However, Syt I, SytII, and SytIX have been shown to control fast neurotransmitter release (Xu, Mashimo et al. 2007). The other members of the family are thought to perform actions similar to these fast synaptotagmins, but in other cellular contexts (Sudhof 2004).

1.5.2 Synaptotagmin VII

Calcium is used as a signaling molecule in a number of systems for regulation of various regulated secretion processes. Synaptotagmin VII is a calcium binding synaptotagmin that has been shown to be involved in exocytosis of glucagon from islets of langerhans as well as secretory granules from PC12 cells (Schonn, Maximov et al. 2008; Gustavsson, Wei et al. 2009). There have also been reports of SytVII being involved in immune function, specifically the fusion of lytic vesicles with endocytosed pathogens (Martinez, Chakrabarti et al. 2000; Gerasimenko, Gerasimenko et al. 2001). However, mice lacking SytVII have no immune deficit, indicating that there may be a problem with these previous studies or that another synaptotagmin is present and can compensate for the loss of SytVII function (Sugita, Han et al. 2001; Maximov, Lao et al. 2008).

Recent unpublished in vivo work from Mingshan Xue and the Rosenmund lab lead to an interesting prospect regarding SytVII. They created a chimeric synaptotagmin using the C2A of Synaptotagmin I and the C2B domain of SytVII. This chimeric synaptotagmin failed to rescue a SytI KO phenotype. This was surprising given the 49% sequence identity between SytI C2B and SytVII C2B. In an effort to restore function of the chimera, residues on the SytVII C2B were mutated to corresponding residues on SytI C2B as determined by sequence alignment. Surprisingly, a now 75% identical C2B domain was still unable to rescue the knockout phenotype. These results suggested that perhaps there is a structural difference between SytVII C2B and SytI C2B and lead to the structural study presented in this work.

1.5.3 Synaptotagmin IX

Synaptotagmin IX is a canonical member of the synaptotagmin family. It is expressed mainly in brain and its function overlaps with SytI and SytII as a sensor for fast neurotransmitter release (Xu, Mashimo et al. 2007). A special subset of neurons in the limbic system and striatum mainly use SytIX as the calcium sensor, making SytIX an important protein for emotional well-being. In this study I will present the crystal structure of the C2A domain of SytIX.

Previous studies showed that the C2A domain of SytIX to be highly similar to that of SytI (Grise, Taib et al. 2007) with sequence identity around

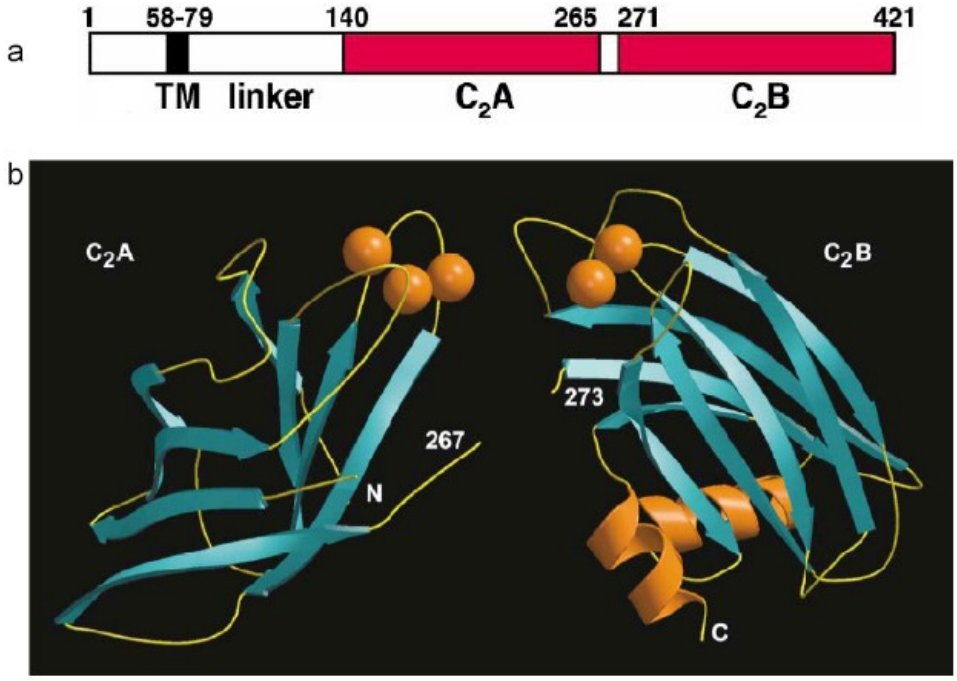

Figure 6 A summary of information on the structure of Synaptotagmin I. (A) The domain structure of Synaptotagmin I with the C2A and C2B domains colored in red. TM stands for transmembrane domain. Note the long linker region. (B) The C2A and C2B domains show a β-sandwich architecture with 4 β-strands on each side of the molecule. Ca^{2+} ions have been modeled as orange spheres.

50%. The C2A domain of SytIX is responsible for translocation of the isoform to the plasma membrane, possibly aided by its calcium dependent phospholipid binding activity(Grise, Taib et al. 2007). However, the C2B domain of SytIX has had a somewhat controversial history, with conflicting reports about its calcium binding activity in the literature (Tucker, Edwardson et al. 2003; Shin, Maximov et al. 2004). More recent published data from the Sudhof lab (Xu, Mashimo et al. 2007) and unpublished data from our laboratory indicate that both the C2A and C2B domains of SytIX bind to phospholipids in a calcium dependent manner.

CHAPTER TWO

INTERACTION OF THE N-TERMINAL REGION OF COMPLEXIN WITH THE SNARE COMPLEX

2.1 Introduction

As previously discussed, the interaction of CpxI with the SNARE complex has been well studied using a variety of methods (Pabst, Hazzard et al. 2000; Reim, Mansour et al. 2001; Bowen, Weninger et al. 2005; Tang, Maximov et al. 2006; Li, Augustine et al. 2007; Chicka and Chapman 2009). Despite the growing list of Cpx papers, the mechanism of Cpx function remains a mystery. Previous studies have frequently used a short construct of complexin, CpxS. Unfortunately the importance of the N-terminal 26 residues of the protein was not known until 2007, when Xue et al showed that removal of the first 26 residues of CpxI abolishes complexin function(Xue, Reim et al. 2007).

It was unclear why the first 26 residues were critical for Cpx function,. We hypothesized that the N-terminal region of complexin interacts with lipids. This interaction would be able to explain previous data from the Shin group that complexin accelerates fusion in a calcium dependent manner in single-vesicle fusion assays(Yoon, Lu et al. 2008). In these assays, single vesicles containing reconstituted SNAREs were shown to fuse quickly in response to calcium, even in the absence of SytI, which is thought to be the calcium sensor for fast

neurotransmitter release(Fernandez-Chacon 2001). With these two studies in mind we set out to investigate the function of the N-terminus in the context of membranes and SNAREs.

2.2 Materials and Methods

2.2.1 Recombinant Protein Production

DNA constructs containing CDNA for expression of the SNARE motifs of Syx, SN1, SN3, CpxFL, and SybS were already available in the lab. These constructs were made by E. Kovrigin, a former postdoctoral fellow in our laboratory. These constructs were transformed into BL21(DE3) *E.coli* cells for expression and kept in glycerol stocks(40% glycerol) at -80°C.

For a typical 1 L culture, a small portion of the glycerol stock was added to 50mL of TB+ 50ug/mL ampicillin and incubated overnight at 37°C. 10mL of the overnight culture was then added to 1L TB containing ampicillin to an OD_{600} of 0.5-0.7, at which point protein expression was induced by the addition of 0.4mM IPTG. After the addition of IPTG, the cultures were incubated at 25°C overnight, after which they were centrifuged at 4000 x g for 30 minutes in a swinging bucket rotor and the pellets were resuspended in 10mL PBS + Sigma inhibitor cocktail(Sigma). The cell suspension was then frozen in liquid nitrogen and stored at -80°C until for further purification.

For experiments requiring isotopic labeling, a similar growth and expression strategy was used. However, M9 minimal media was used as the growth medium instead of TB. 1L of M9 minimal media contains 6.8 g Na_2HPO_4, 0.5 g NaCl, 1.0 g NH_4Cl, 3.0 g KH_2PO_4, 2.0 mM $MgSO_4$, 100 *u*M $CaCl_2$, and 4.0 g D-(+)-glucose. For experiments that required ^{15}N labeled protein, $^{15}NH_4Cl$ was used instead of the standard $^{14}NH_4Cl$.

Thawed cell suspensions were passed through a cell disruptor (Emulsiflex C-5) at 10,000 psi 3 to 4 times to lyse the cells. The lysate was then cleared by centrifugation at 19,000 x g in a JA-20 rotor for 30 minutes. The supernatant was then filtered using a 0.45µm syringe filter and 1.5mL glutathione sepharose (GS4B) beads were added. The mixture was then rotated for 16 hr at 4°C or 2hr at room temperature to allow the glutathione-S-transferase to bind to the affinity beads. The resulting mixture was then run through a gravity flow chromatography column (Bio Rad), thus allowing non-binding proteins to flow through. The beads were then successively washed with 250mL PBS containing 1% triton X-100, 1M NaCl, and no salt PBS. At this point the beads were washed with benzonase buffer (20mM Hepes, 100mM NaCl, 2 mM $MgCl_2$) and then incubated for 2 hours at room temperature with 10 units/mL benzonase nuclease to digest bound nucleic acids. After benzonase disgestion, the beads are washed with thrombin cleavage buffer (50mM Tris pH 8.0, 150mM NaCl, 2 mM $CaCl_2$) and then incubated for two hours at room temperature with 5-7 units of thrombin

per mL of thrombin buffer-beads mixture to cleave the GST tag from the protein. The flow through was collected and run over a Superdex 75 HiLoad 16/60 size exclusion chromatography column. In the cases of SyxS and SybS, a further ion exchange chromatography step was performed (Source Q and Source S, respectively). Otherwise protein concentration was assessed using SDS-PAGE and UV_{280}, and then proteins were aliquoted, frozen in liquid nitrogen, and stored at -80°C. A typical yield was 3-5 mg per liter of culture.

For co-expressed full length Syntaxin-SNAP25, plasmids containing the CDNA for both SNAP25 and full length syntaxin were transformed into BL21 (DE3) cells and then grown on a plate containing both kanamycin and ampicillin to select for colonies that contain both the Syntaxin and SNAP25 plasmids. Single colonies were then transferred to an overnight culture containing both antibiotics. The next day, 10mL of this culture was transferred to 1L of LB containing both antibiotics. Cells were then incubated at 37°C until the OD_{600} reaches 0.6-0.8, at which point 1mM IPTG was added. Induction of protein expression then continues for 15 hours at 25°C. At this point, the cultures are centrifuged at 4000 x g and resuspended in breaking buffer A. The cells were incubated with 1% Triton X-100 for 30 minutes to solubilize full-length syntaxin. The suspension was then passed through the cell disruptor at 10,000psi 4-5 times. The resulting lysate was centrifuged at 20,000 x g. The supernatant was then added to a slurry of 1.5mL Ni-NTA beads (Qiagen) per liter of culture and

incubated overnight at 4°C. The mixture was then put through a gravity flow column to allow unbound proteins to flow through the beads. The beads were then washed with 250mL Buffer A and Buffer B. At this point, the detergent is changed to β-OG by washing the beads 3 times with 10mL of 1% β-OG containing thrombin cleavage buffer. After these washes, the beads are incubated with 1% β-OG containing thrombin cleave buffer containing 5-7 units/mL of thrombin at room temperature for 2 hours. After the thrombin has cleaved both affinity tags from the coexpressed proteins, they can be eluted from the column. After cleavage, the eluate is subjected to ion exchange chromatography (MonoQ) using 50mM Tris pH 8.0, 2mM DTT, and 1% β-OG as buffer A and 50mM Tris pH 8.0, 2mM DTT, 1M NaCl, and 1% β-OG as buffer B. Purity and stoichiometry of the complex was then assessed by SDS-PAGE, and concentration was determined by UV_{260} absorbance. The extinction coefficient used in this calculation is the addition of the individual coefficients.

2.2.2 Formation of SNARE complexes

SNARE complexes were formed using either SNARE fragments, or coexpressed SyxFL+SNAP25. In the case of SNARE fragments, the order in which the components are mixed is extremely important, due to the formation of a kinetically trapped SN1-SyxS species. First SyxS is mixed with SN3 and Syb. After a few minutes SN1 can be added to the mixture, which is then incubated

overnight at 4°C. Complex formation was assessed by SDS-PAGE comparing samples boiled for 10 minutes and unboiled samples.

In the case of SNARE complexes that include the transmembrane domain of SyxFL, special care was taken to add 1% β-OG to SybS before it was added to the coexpressed SyxFL+SNAP25. The resulting mixture was then incubated at 4°C overnight. Complex assembly was assessed by SDS-PAGE of both boiled and unboiled samples.

2.2.3 Preparation of Liposomes by Extrusion

Liposomes used for these experiments were created using an 85:15 molar ratio of POPC: DOPS, except for experiments where dansyl-DPPE lipids were used, in which case a ratio of 82:15:3 POPC:DOPS:Dansyl-DPPE was used.. All lipids were obtained from Avanti polar lipids and kept in chloroform at -20°C until used. 15mM lipid was dried on a borosilicate tube under a nitrogen stream into a thin film. The film was created by holding the tube at an angle so that the chloroform is spread out over a large area of the tube upon rotation. The resulting lipid film is then dried under vacuum for 2 hours at room temperature. The lipid film was then rehydrated with 200µL of reconstitution buffer (25mM HEPES pH 7.1, 100mM KCl, 2mM DTT) and vortexed for 5 minutes. The mixture was then subjected to 5 freeze/thaw cycles in liquid nitrogen to prevent membrane fouling. The mixture was then warmed for 1 min in a 37°C water bath to ensure that the

mixture is above the T_m of the lipids being used to prevent formation of a gel during extrusion. The lipid suspension was then passed through an 80nm pore size filter 31 times. After extrusion the liposomes were subjected to dynamic light scattering to assess their homogeneity and size.

2.2.4 Reconstitution of SNARE Complexes into Liposomes

With both the SNARE complex and liposomes prepared, reconstitution was performed using the so-called "Direct Method"(Chen, Arac et al. 2006), in which detergents begin to saturate the liposomes and soften them, which allows for the insertion of the transmembrane domain of SyxFL. The SNARE complexes and liposomes were mixed in a 2:1 ratio, in order to obtain a final β-OG concentration of 0.66% and a protein: lipid ratio of at least 1:1000. The mixture was then rotated for 30min at room temperature. Detergent was removed by extensive dialysis. In total, 4L of reconstitution buffer containing 1g/L SM2 Bio-Beads was used. This total is broken up into three separate steps. The first two steps are for 1hr each, and use 1L of buffer each. The final dialysis step is 2L and lasts 16 hours. After the final dialysis, the quality of the liposomes was assessed by DLS. In order to determine the concentration of SNARE complexes reconstituted in the correct direction, a titration using CpxS-Bodipy was performed using fluorescence anisotropy.

2.2.5 NMR Spectroscopy

Proteins were purified as previously described in this chapter. All spectra were recorded on INOVA600 spectrometers (Varian). ^{1}H-^{15}N HSQC experiments were performed on complexin in the presence of SNARE proteoliposomes, liposomes, and soluble SNARE complexes. For all experiments involving reconstituted SNARE proteoliposomes or plain liposomes, the concentration of CpxI was 2μM and the SNARE complex concentration was 5μM. For experiments involving soluble SNARE complexes, the concentrations were increased to 60μM CpxI and 140μM SNARE complex for increased sensitivity and decreased acquisition time. All data were processed using nmrPipe and visualized using the program NMRViewJ.

2.2.6 Fluorescence Measurements

Full-length complexin contains one natural cysteine residue at position 105. To ensure that my complexin was specifically labeled on the N-terminus, I mutated C105 to serine, and residue A12 to cysteine using the standard Quickchange Mutagenesis Kit (Stratagene). The mutant protein was purified using the same method described in section 2.2.1 for full length CpxI, except TCEP was used as a reducing agent instead of DTT.

The labeling reaction was carried out by adding a tenfold molar excess of NBD-iodoacetamide (Molecular Probes) to a solution of 50μM $Cpx^{A12C, C105S}$.

The reaction was shielded from light and allowed to proceed overnight at 4°C. The reaction was halted by adding 5mM DTT. Unreacted dye was removed using a PD-10 desalting column followed by dialysis against 4L of 25mM HEPES pH7.1 100mM KCl for 4 hours. The labeling efficiency of the dye was calculated by dividing the moles of dye divided by the moles of protein. Amounts of dye and protein were determined using a UV-Vis spectrophotometer (HP) and comparing the absorbance of the dye at 485nm to the absorbance at 280nm. Labeling efficiency was calculated to be between 85-100%.

Experiments were carried out in triplicate using three separate preparations of protein, SNAREs, and liposomes. All spectra were acquired on a PTI fluorimeter at room temperature. Before any measurements were made, a standard sample of 100nM $Cpx^{A12C, C105S}$-NBD was used to ensure that the slit widths of the instrument were adjusted to give an emission intensity of 180,000 counts at 550nm when excited at 485nm. All components were buffer exchanged into reconstitution buffer (20mM HEPES pH7.1, 100mM KCl, 1mM TCEP) before mixing. Experiments contained 100nM $Cpx^{A12C, C105S}$-NBD and either 2mM Lipid, 10μM soluble SNARE complex, or 5μM liposome reconstituted SNARE complex.

2.3 Results

The ^{1}H-^{15}N HSQC experiment is a useful tool that can quickly identify binding sites. As was mentioned previously, this experiment reports on each residue in a protein, allowing simple identification of interacting residues by looking for chemical shift changes or changes in the intensity of crosspeaks. I used the HSQC to look for interactions between the N-terminal residues of CpxI and proteoliposomes containing reconstituted SNARE complexes. Since CpxI is an inherently disordered protein, it was possible to work at very low concentrations of 2μM while still obtaining excellent spectra over a 12 hour acquisition. To start out, we wanted to see if there was some interaction of the CpxI N-terminus with reconstituted SNARE complexes. The CpxFL spectra shown in black (**Figure 7**) is similar to previous reports(Pabst, Hazzard et al. 2000) and indicates that CpxI is unfolded by itself in solution due to the poor dispersion of crosspeaks between 8-8.6 ppm in the ^{1}H dimension.

The experiments shown in **Figure 7** demonstrate that there is an interaction between the N-terminal residues of complexin and the SNARE proteoliposomes. Clear broadening was observed for a number of peaks, including those from both the N-terminus (Residues M5, K6, A8, and A12) [**Figure 7**] and the canonical SNARE binding α-helix. However, this experiment could not show which components present in the sample were sufficient for binding. This led to three possible options for the identity of the binding partner for the N-terminus of complexin. The N-terminus could bind to either SNAREs,

lipids, or SNAREs and lipids simultaneously. In order to test these possibilities I used a combination of NMR and fluorescence spectroscopy.

Testing the interactions with SNAREs and lipids was relatively simple using standard NMR spectroscopy. I employed the ^{1}H-^{15}N HSQC to show that in the presence of >1000x lipid, resonances on CpxI are unaffected, indicating that there is no interaction between liposomes and CpxI (**Figure 8**). A HSQC spectrum of ^{15}N CpxI was then recorded in the presence of excess soluble SNARE complexes composed of SyxS, SybS, SN1, and SN3. In this spectrum clear broadening was observed for residues in the N-terminus as well as the SNARE binding region (**Figure 9**). These two experiments suggest that the N-terminus primarily binds to the SNARE complex, but it does not preclude the possibility that either a CpxI-SNARE complex can interact with lipids, or that the interaction of CpxI with the SNARE complex increases the local concentration of CpxI near the membrane and facilitates interaction with lipid.

In order to test this possibility, I designed a cysteine mutation on the N-terminus of CpxI that allowed the attachment of a fluorescent NBD probe. This fluorophore has low fluorescence in aqueous environments and high fluorescence in hydrophobic environments(Lakowicz 2006). If indeed CpxI interacts with membranes, there should be an increase in fluorescence intensity upon addition to SNARE-reconstituted proteoliposomes that is not present under conditions with soluble SNARE complexes alone. As Figure 10 clearly shows, the fluorescence

intensity of both the SNARE proteoliposome and soluble SNARE complex containing samples have very similar intensities, indicating that the N-terminus is not binding to membranes in addition to the SNARE complex.

These results clearly show an interaction of the CpxI N-terminus with the SNARE complex. However, in order to show biological relevance of this interaction I needed to create a small mutation that blocks the activity of the N-terminus *in vivo* while showing clear disruption of the N-terminus-SNARE complex interaction *in vitro*. This presented a problem, since we have no structural information about the N-terminus when it is bound to the SNARE complex. In an effort to understand what the structure of the N-terminus might be and create point mutations, I submitted the sequence of complexin to a secondary structure prediction algorithm called PSIPred(Mcguffin, Bryson et al. 2000). The program returned that the N-terminus should be an α-helix. Although previous NMR data shows that complexin is unstructured by itself in solution, it is possible that upon interaction with the SNARE complex the N-terminus folds into a helix. Using this prediction I created a helical wheel (**Figure 11**) model of the N-terminus. This helical wheel model showed the N-terminus as an amphipathic helix.

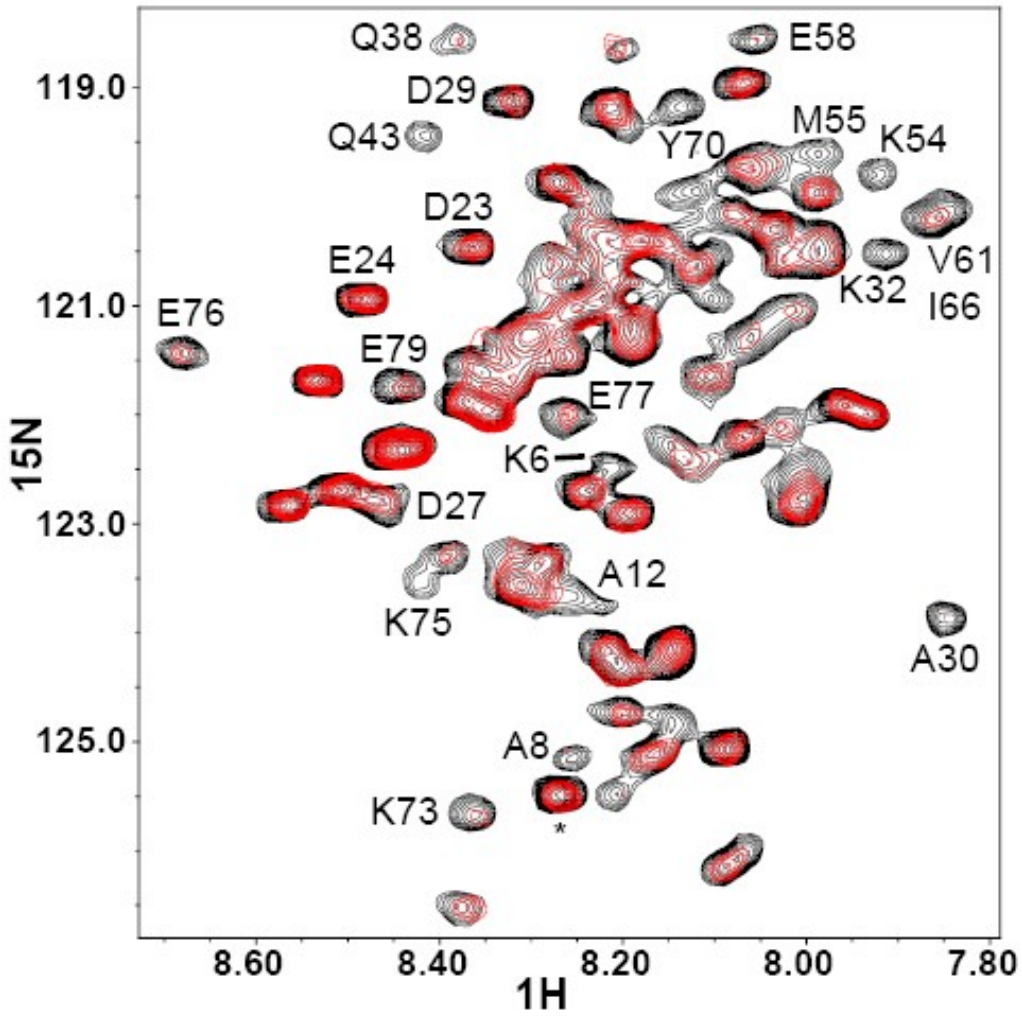
Q38
E58
D29
Q43
Y70
M55
K54
D23
E24
V61
K32
I66
E76
E79
E77
K6
D27
A12
K75
A30
A8
K73
*
119.0
121.0
123.0
125.0
15N
8.60
8.40
8.20
8.00
7.80
1H

Figure 7 ^{1}H-^{15}N HSQC spectra of CpxFL shows binding of the N-terminus to SNARE proteoliposomes without Ca2+. The black spectrum is WT CpxFL alone at 2μM. The red spectrum is 2μM WT CpxFL in the presence of excess liposome-reconstituted SNARE complexes. Samples were prepared in 20mM HEPES pH 7.1 with 100mM KCl and 2mM TCEP with 1mM EDTA. Spectra were acquired for 12 hours at 25°C. Labeled residues in the N-terminus such as M5, K6, A8, and A12 show significant broadening, indicating binding to SNARE proteoliposomes.

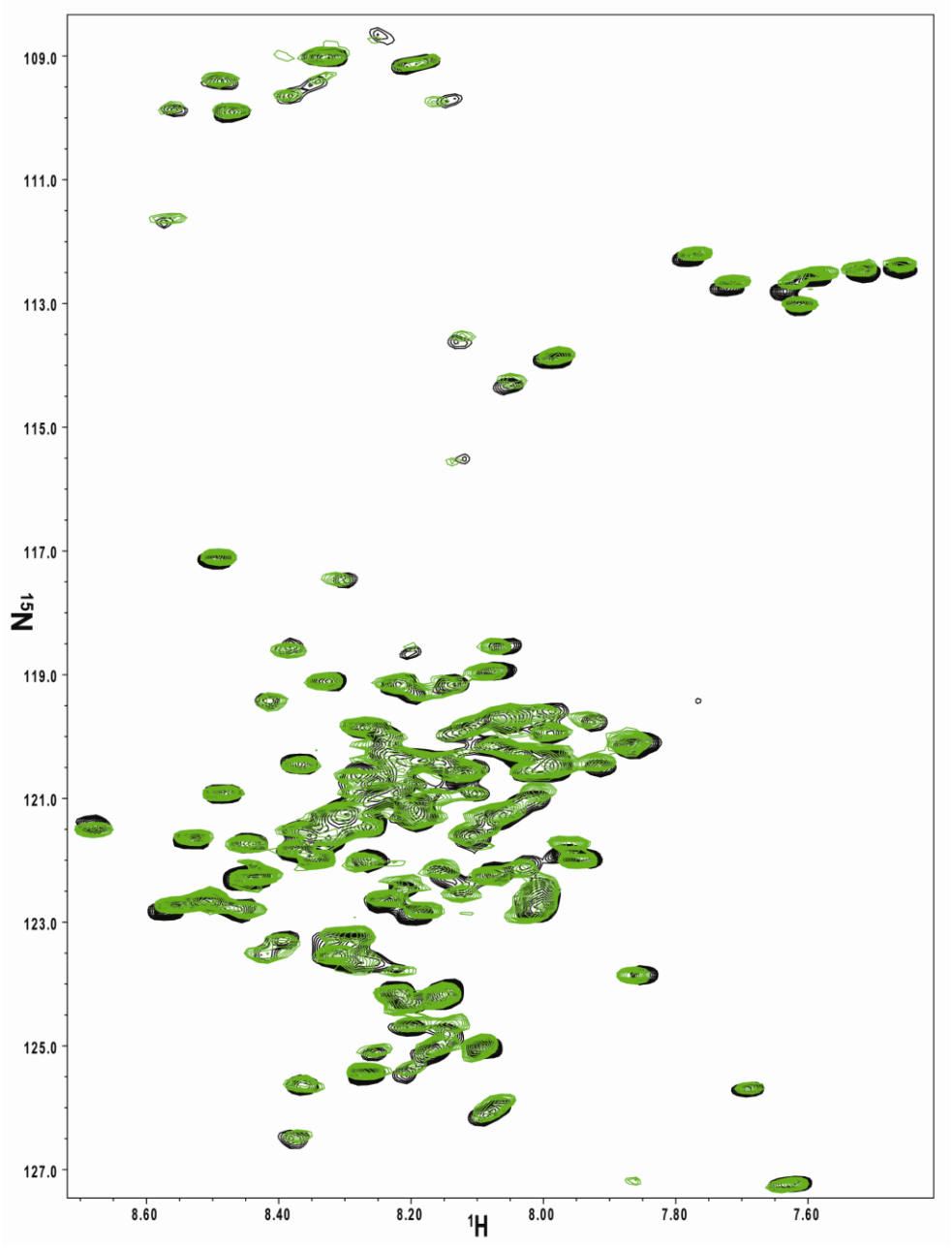
109.0
111.0
113.0
115.0
117.0
119.0
121.0
123.0
125.0
127.0
N_{15}
8.60
8.40
8.20
8.00
7.80
7.60
^{1}H

Figure 8 Overlay of ^{1}H-^{15}N HSQC spectra from 2μM Complexin alone (**Black**) and in the presence of 1mM liposomes (**Green**). Samples were prepared in 20mM HEPES pH 7.1 with 100mM KCl and 2mM TCEP with 1mM EDTA. Spectra were acquired for 12 hours at 25°C. The superimposable spectra clearly show that there are no changes in the chemical shifts of residues in CpxI.

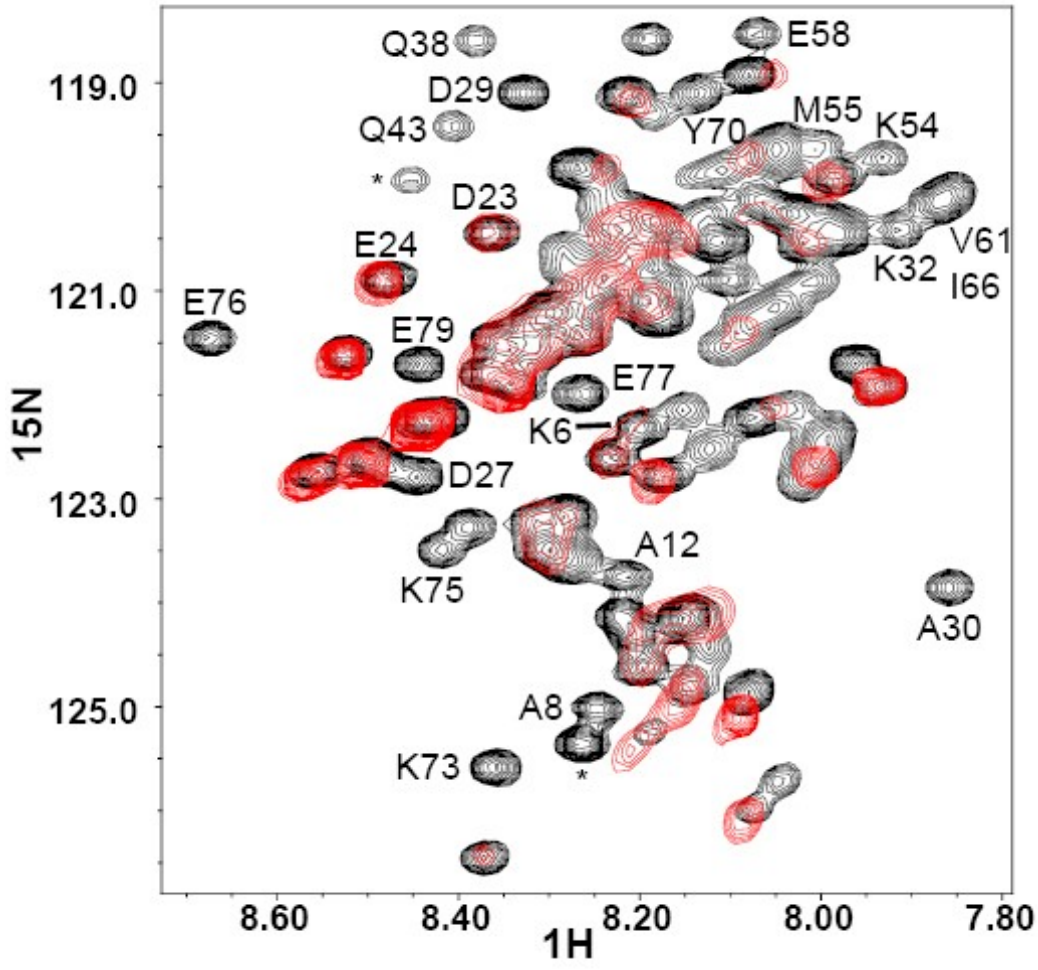
Q38
E58
D29
Q43
Y70
M55
K54
D23
E24
V61
K32
I66
E76
E79
E77
K6
D27
A12
K75
A30
A8
K73
119.0
121.0
123.0
125.0
15N
8.60
8.40
8.20
8.00
7.80
1H

Figure 9 Overlaid 1H-15N HSQC spectra of 60μM complexin alone (**Black**) and in the presence of 140μM soluble SNARE complexes (**Red**). Samples were prepared in 20mM HEPES pH 7.1 with 100mM KCl and 2mM TCEP with 1mM EDTA. Spectra were acquired for 6 hours at 28°C. Two groups of crosspeaks are selectively broadened upon SNARE binding; those in the central SNARE binding α-helix, and a group located in the N-terminal region of complexin. N-terminal peaks M5, K6, A8, A12 are all completely broadened indicating binding of the N-terminus to the soluble SNARE complex.

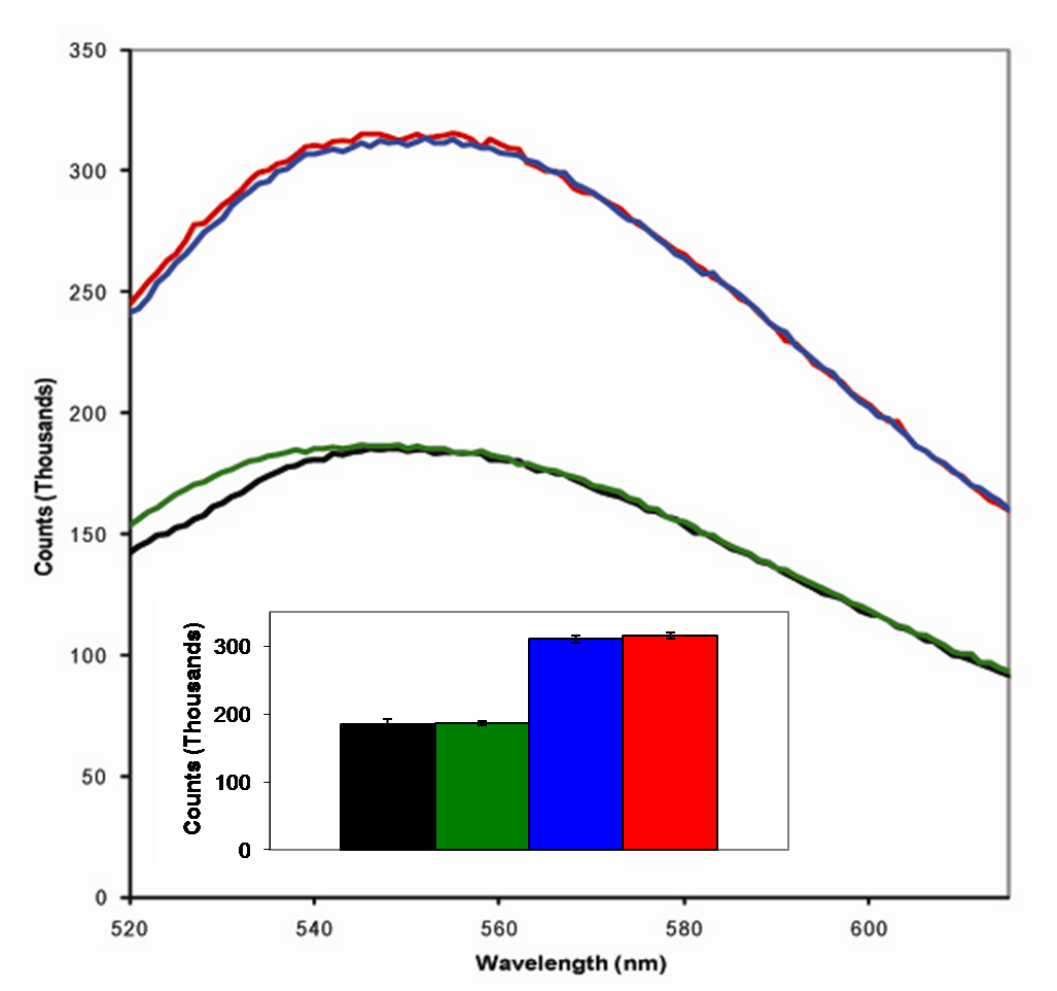
350
300
250
200
150
100
50
0
Counts (Thousands)
520
540
560
580
600
Wavelength (nm)
300
200
100
0
Counts (Thousands)

Figure 10 Fluorescence measurements reveal a single binding mode of the CpxI N-terminus. Fluorescence intensities of 100nM Cpx$^{A12C, C105S}$-NBD alone (**Black**) are very similar in the presence of 1mM liposomes (**Green**), indicating that there is no interaction of the NBD probe with the hydrophobic environment of the lipid. Upon binding to 10μM soluble SNARE complexes (**Red**), the NBD signal increases, but does not increase further upon binding to reconstituted SNARE proteoliposomes (**Blue**). The lack of any difference between soluble and reconstituted SNARE complex samples indicates that the N-terminus does not interact with lipid, even in the presence of reconstituted SNARE complexes.

This result allowed me to create a double mutant that would destroy the amphipathic character of the helix by the mutation of only two residues. I chose to add a negative charge to the center of the hydrophobic side on the helix by mutating methionine 5 to glutamic acid (M5E). In addition, I reversed the charge on lysine 6, again by mutating to glutamic acid (K6E). In order to test the hypothesis that the amphipathic character of the helix is the structural basis for the importance of the N-terminal interaction with the SNARE complex, I produced ^{15}N labeled CpxMKEE for use in NMR experiments.

Previous evidence has shown that CpxI is not folded in solution, so creating two point mutants should not have any effect on the overall fold of complexin in solution. Indeed this prediction is born out in ^{1}H-^{15}N HSQC of CpxMKEE, which overlaps well with CpxFL, except for the crosspeaks corresponding to residues immediately surrounding the site of mutation (**Figure 12**).

The next experiment was to test if the MKEE mutation disrupted N-terminus binding to the SNARE complex. To measure binding of the MKEE N-terminus to reconstituted SNARE proteoliposomes I recorded a ^{1}H-^{15}N HSQC and compared it to spectrum of CpxI+SNARE proteoliposomes. By overlaying the two spectra, it became obvious that the new peaks created by the mutation were not broadened by SNARE proteoliposome binding (**Figure 13**). Additionally, residues in the central SNARE-binding α-helix of complexin were still broadened,

indicating that the MKEE mutation abolishes the interaction of the N-terminus while leaving the central α-helix binding unaffected as evidenced by crosspeak broadening of residues outside the N-terminus.

The interaction between the SNARE complex and the N-terminus of CpxI is critical for fusion *in vivo*. Work done in collaboration with our laboratory by Mingshan Xue from Christian Rosenmund's laboratory in regards to the CpxI N-terminal interaction has shown that the MKEE mutant CpxI cannot rescue the CpxI I/II DKO phenotype (**Figure 14)**. The probability of vesicular release is a combination of both the number of docked vesicles, as well as the size of evoked EPSCs. **Figure 14** clearly shows a profound defect in P_{vr} caused by the MKEE mutation. Because we knew from in vitro data (**Figures 7, 9, 10, 13**) that the N-terminus of Cpx interacts with the SNARE complex, and this interaction is disrupted by the MKEE mutation, we hypothesized that perhaps the SNARE complex is not completely zippered at the C-terminus in the presence of MKEE. If this were the case, there should be an effect on the ready releasable pool (RRP) size because a more stabilized SNARE complex should provide energy to overcome the energy barrier of fusion. However complete knockout of CpxI/II/III does not display a particularly severe phenotype in an assay using 500mM sucrose to measure the size of the RRP (**Figure 15**). However, upon using 250mM sucrose, it becomes clear that there are two populations of vesicles that can be fused by 500mM sucrose (**Figure 16**).

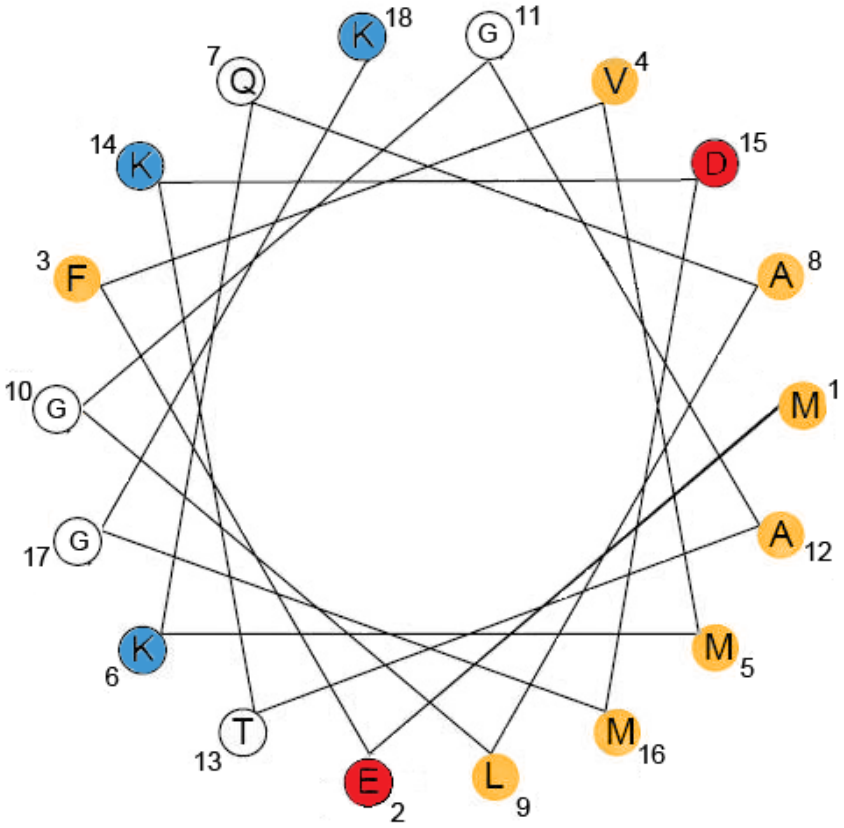
K 18
G 11
7 Q
V 4
14 K
D 15
3 F
A 8
10 G
M 1
17 G
A 12
K 6
M 5
T 13
M 16
E 2
L 9

Figure 11 A helical wheel model of the N-terminus of CpxI. The N-terminus forms a clear amphipathic helix, with a patch of hydrophobic residues (**Orange**) bordered by negatively charged residues (**Red**), with positively charged residues on the opposite side (**Blue**).

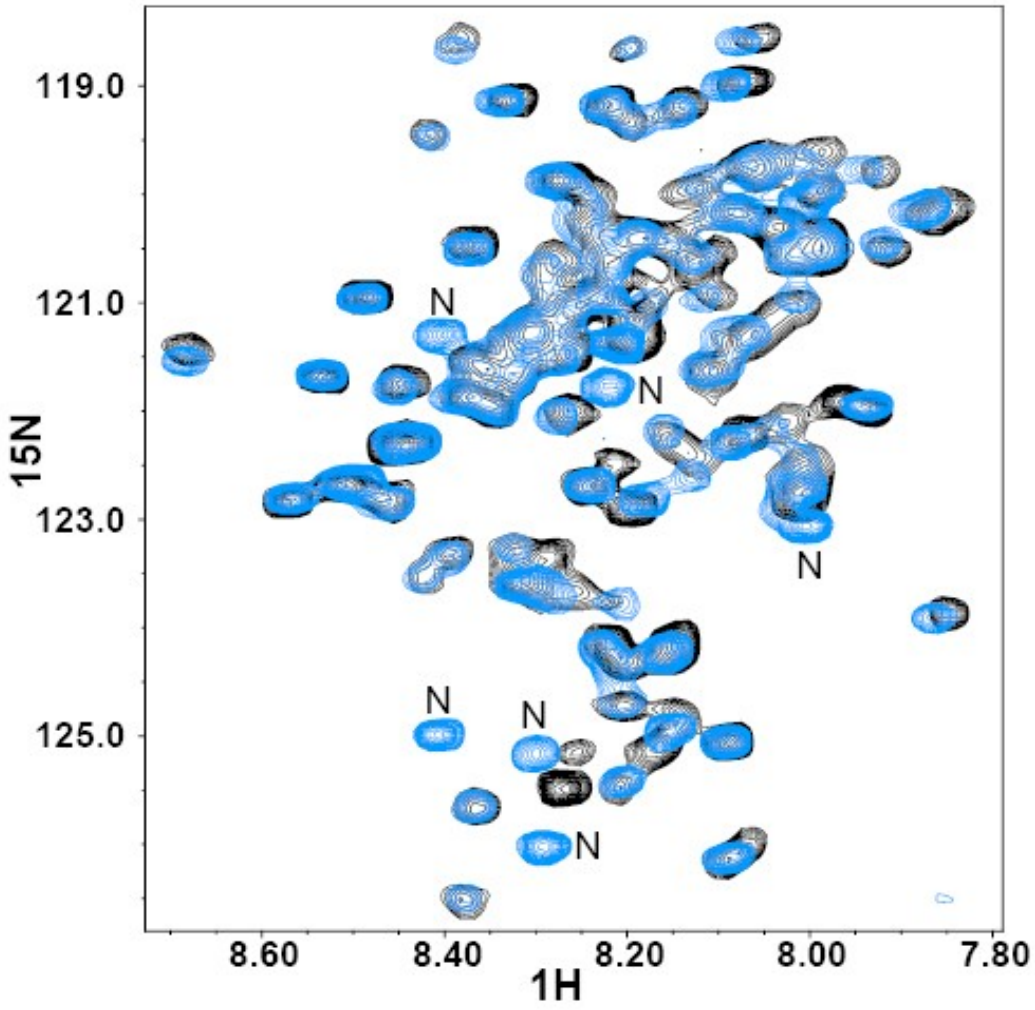
119.0
121.0
123.0
125.0
15N
N
N
N
N
N
N
8.60
8.40
8.20
8.00
7.80
1H

Figure 12 ^{1}H-^{15}N HSQC spectra show that the overall unfolded structure of CpxI has not been perturbed by the mutation of residues 5 and 6. 2μM Wild type CpxFL (**Black**) is clearly unfolded, and the spectrum of 2 μM CpxMKEE (**Blue**) clearly overlaps with that of the WT. New crosspeaks that resulted from the mutation of residues M5 and K6 to E are marked with the letter "N". Both spectra were acquired for 12 hours at 28°C in 20mM HEPES pH 7.1, 100mM KCl, 2mM TCEP.

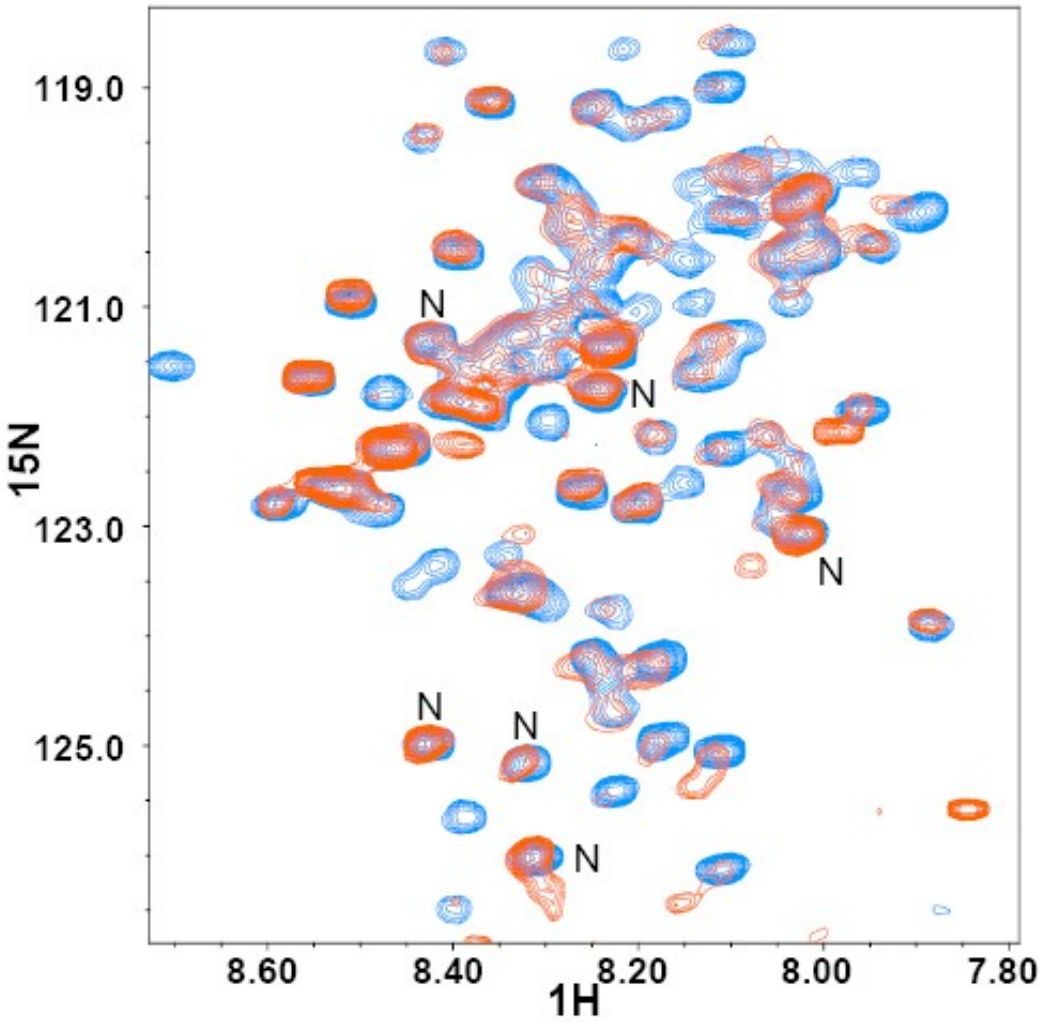
119.0
121.0
123.0
125.0
15N
N
N
N
N
N
N
8.60
8.40
8.20
8.00
7.80
1H

Figure 13 ^{1}H-^{15}N HSQC spectra of CpxI and MKEE mutant shows the disruption of N-terminus binding to the SNARE complex. Overlaid spectra of 2µM ^{15}N CpxFL (**Blue**) or 2µM ^{15}N MKEE (**Orange**) in the presence of 5µM liposome reconstituted SNARE complexes reveals a set of peaks (labeled 'N') corresponding to residues near the MKEE mutation that no longer bind to the reconstituted SNARE complex. Spectra were recorded for 12 hours at 25°C in 20mM HEPES pH7.1, 100mM KCl, and 2mM TCEP.

The MKEE mutant shows a deficit in 250mM sucrose response when compared to wild type (**Figure 16**) indicating that complete zippering of the SNARE complex may be facilitated by the interaction of the N-terminus with the C-terminus of the SNARE complex. When taken together, the In vivo data from Mingshan and In vitro data from my work reveal a novel step in the priming process.

2.4 Discussion and Significance

Complexin is a complicated regulator of neurotransmitter release. The dual role of complexin in neurotransmitter release has recently been an issue of some contention, with some indicating a negative role in neurotransmitter release, whereas others take into account multiple types of data that show complexin be both an inhibitor and a facilitator at different points in the neurotransmitter release process (Chen 2002; Tang, Maximov et al. 2006; Xue, Reim et al. 2007; Giraudo, Garcia-Diaz et al. 2008). The results presented here clearly show that there is an interaction between the N-terminus of CpxI and the SNARE complex, a novel finding. Other previous papers have suggested from mutational studies that the N-terminus may interact with the membrane-proximal region of Syb (Maximov, Tang et al. 2009). The fluorescence and NMR data presented here contradict the idea that the N-terminus of CpxI contacts membranes that was suggested by a

number of groups (Xue, Reim et al. 2007; Maximov, Tang et al. 2009). Additionally, there has been speculation in the literature that CpxI interacts with lipid through a C-terminal amphipathic helix. The liposome floatation assay used by F. Seiler et al(Seiler, Malsam et al. 2009) is directly contradicted by the more detailed NMR data in **Figure 8**.

The results presented here fit nicely with the model proposed by our laboratory in 2002 that (Chen, Tomchick et al. 2002) CpxI promotes fusion through its stabilizing effect on the SNARE complex. What was not known at the time is that CpxI interacts with the SNARE complex in three distinct binding modes, and that the N-terminal interaction of Cpx with the C-terminus of the SNARE complex is critical for the function of CpxI. The model now proposed is shown in **Figure 17**. The central α-helix binds to the SNARE complex with high affinity and stabilizes the N-terminal side of the SNARE complex while simultaneously providing a scaffold for the interactions of both the N-terminus and the accessory helix. The accessory helix can substitute for the C-terminal half of Syb and inhibit fusion and full zippering of the SNAREs. The N-terminal interaction occurs after inhibition by the accessory helix has been released by a protein-protein interaction with an as of yet unknown partner. With the accessory helix displaced, the N-terminus most likely helps to stabilize the fully-assembled SNARE complex. It is now becoming evident that priming is at least two

Pvr

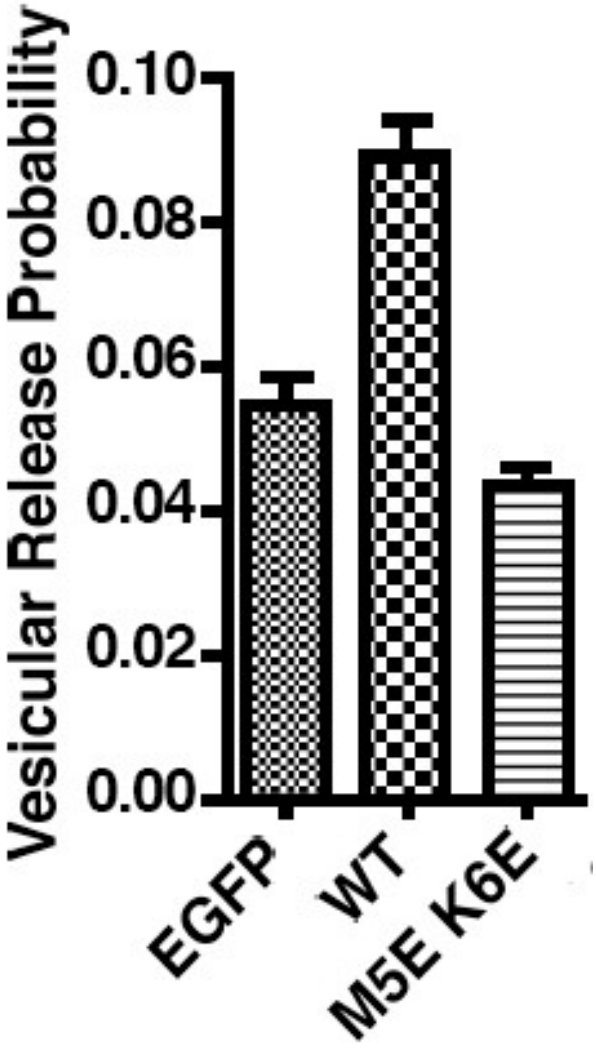
Vesicular Release Probability
0.10
0.08
0.06
0.04
0.02
0.00
EGFP
WT
M5E K6E

Figure 14 Probability of vesicular release (P_{vr}) for Cpx I/II DKO neurons expressing transfected constructs. EGFP was transfected by itself as a negative control. WT Cpx shows full rescue of the KO phenotype, whereas the MKEE mutant shows no rescue. All experiments were performed by Mingshan Xue in Christian Rosenmund's Laboratory.

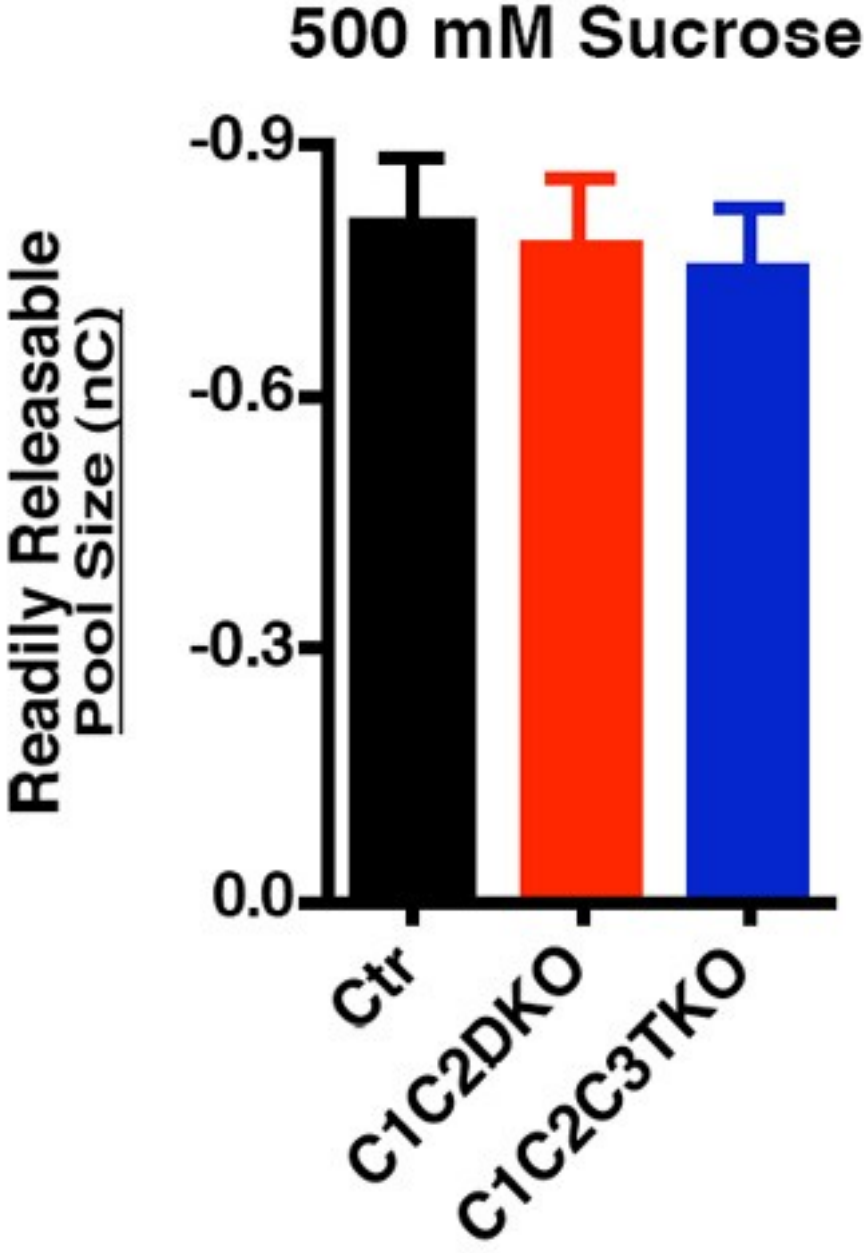
500 mM Sucrose
Readily Releasable
Pool Size (nC)
-0.9
-0.6
-0.3
0.0
Ctr
C1C2DKO
C1C2C3TKO

Figure 15 Complexin I/II and I/II/III KO shows no deficit in 500mM sucrose response. WT Cpx neurons (**Black**), as well as CpxI/II double knockout, and CpxI/II/III triple knockout neurons show no change in response to 500mM hypertonic sucrose, which osmotically fuses primed vesicles. All experiments were performed by Mingshan Xue in Christian Rosenmund's Laboratory.

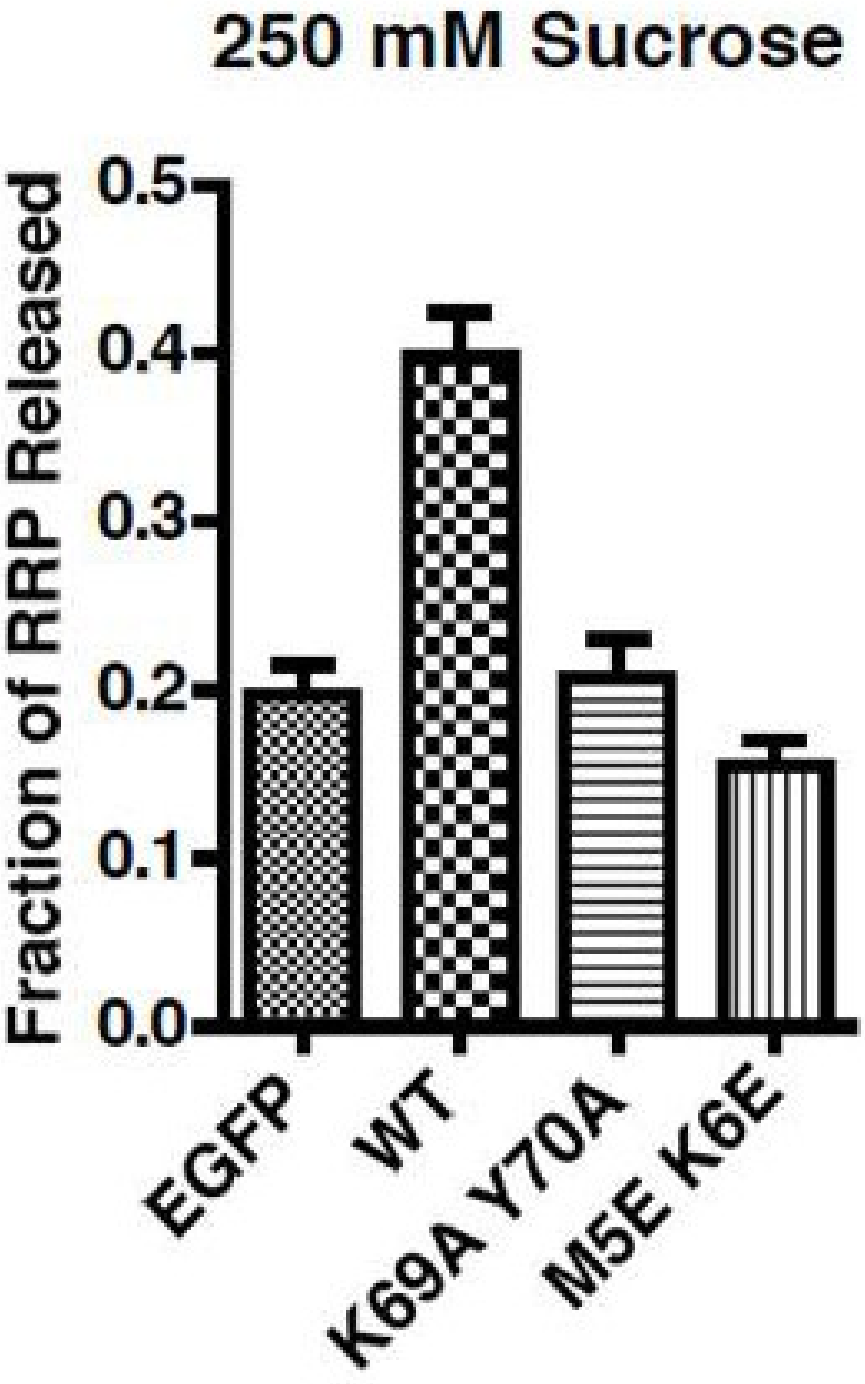
250 mM Sucrose
Fraction of RRP Released
0.5
0.4
0.3
0.2
0.1
0.0
EGFP
WT
K69A Y70A
M5E K6E

Figure 16 250mM Sucrose response reveals a sub-population of vesicles that are incompletely primed. 250mM sucrose was applied to CpxI/II DKO neurons transfected with various expression constructs and the ready releasable pool size was measured using electrophysiological methods. EGFP was transfected into cells as a negative control. Wild type CpxI rescued the KO phenotype completely. The mutation carried by $Cpx^{K69A,Y70A}$ is known to abolish binding to the SNARE complex. In agreement with previous work (Xue, Reim et al. 2007), SNARE binding is necessary for the function of the Cpx N-terminus. The MKEE mutant shows a profound defect in 250mM sucrose competent releasable pool size. All experiments were performed by Mingshan Xue in Christian Rosenmund's Laboratory.

different stages, and that these stages may be dependent on the mode of complexin interaction with the SNARE complex. If the interaction of the accessory helix predominates, the stage is called priming. If the N-terminal interaction predominates, the stage has been coined as "Superpriming" (Maximov, Tang et al. 2009). Each of the three interactions of complexin plays a specific role in regulating neurotransmitter release either positively or negatively, showing that complexin truly is the double edged sword of neurotransmitter release.

Although this work does shed light on the interaction partner of the N-terminus of Cpx, a number of questions remain. According to the model in **Figure 17**, the binding mode of the accessory helix changes upon SNARE zippering and Cpx N-terminus binding. It would be interesting to obtain structural and biochemical data examining the exchange between these two states, as well as the regulation of these two states, perhaps by Syt. The structure of a Complexin-SNARE complex including the N-terminus of complexin has not yet been solved and could provide insight into the energetics of binding and the overall structure of the neurotransmitter release machinery.

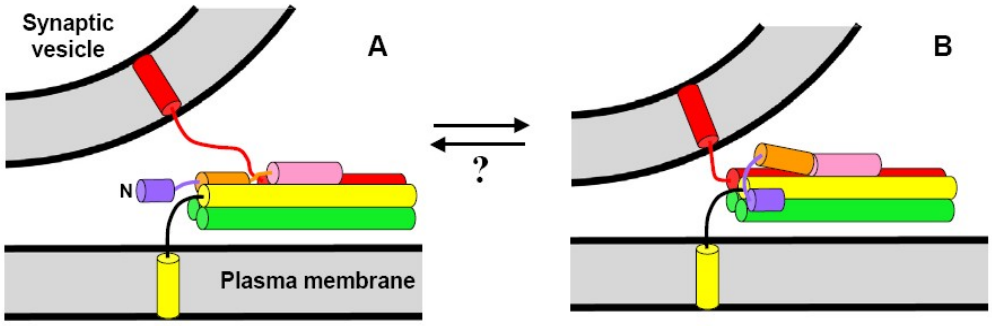

Figure 17 Proposed model of Cpx function. The SNARE complex composed of Syntaxin (**Yellow**), SNAP25 (**Green**), and Syb (**Red**) is shown in complex with Cpx. The central α-helix of Cpx (**Pink**) binds to the SNARE complex, while in part A) the accessory helix (**Orange**) takes the place of the C-terminus of Syb on the SNARE complex, inhibiting release. When the accessory helix is displaced by Syb in B), the N-terminus of Cpx (**Purple**) binds back to the C-terminus of the SNARE complex, stabilizing the complex and lowering the energy barrier for fusion. This N-terminal interaction with the SNARE complex is disrupted by the MKEE mutation, which would explain the deficit in 250mM sucrose release. In this model part A would be considered the "Primed" state whereas part B would be the "Superprimed" state.

CHAPTER 3

CRYSTAL STRUCTURE OF THE C2B DOMAIN OF SYNAPTOTAGMIN 7 AND C2A DOMAIN OF SYNAPTOTAGMIN 9

3.1 Introduction

There have been 16 genes identified that encode for synaptotagmins(Sudhof 2002). This large number indicates that these molecules are probably involved in a variety of membrane fusion events. Synaptotagmin VII has been shown to be the calcium sensor for glucagon exocytosis in the pancreas (Gustavsson, Wei et al. 2009), as well as being the predominant calcium sensor in chromaffin cell exocytosis(Schonn, Maximov et al. 2008).

The Synaptotagmin VII C2B has previously been shown to bind to Ca^{2+} and negatively charged phospholipids, much like Synaptotagmin I (Maximov, Lao et al. 2008). In fact, the sequence identity between the SytI C2B and the SytVII C2B is nearly 50%. This high degree of similarity led our collaborators in the Rosenmund lab to create a SytI C2A-SytVII C2B chimera. They then used this chimera to attempt to rescue SytI KO neurons. Surprisingly, they discovered

that the chimeric protein cannot rescue the KO phenotype. Extensive mutation of nearly 25% of the SytVII C2B domain to corresponding residues on SytI failed to rescue as well (**Table 1**). After the localization and expression of the chimeras was checked, one of the only remaining explanations for this behavior was that SytVII C2B is

3.2 Materials and Methods

3.2.1 Recombinant Protein Expression and Purification

The CDNA construct of SytVIIC2B was a gift from the Sudhof lab. The Sudhof lab construct was transferred to the pGEX-KT expression vector and transformed into BL21 (DE3) cells. After selection on ampicillin containing media, a single colony was transferred into 50mL LB Broth with 50ug/mL Ampicillin and grown overnight. A small amount of the resulting overnight culture was mixed 1:1 with 80% glycerol and frozen at -80 as a glycerol stock. 10mL of the remaining overnight culture was used to inoculate 1L LB Broth containing ampicillin. This larger culture was grown at 37°C until the OD_{600}=0.5-0.7, at which point the temperature was lowered to 25°C and 1mM IPTG was added. Induction was allowed to continue for 16 hours, at which point the culture was spun at 4,000x g. The pellets were resuspended in 200mM Tris 400mM NaCl containing sigma inhibitor cocktail and 5mM EDTA. Resuspended pellets were frozen at -80°C for later use.

Mutation	**Rescue Experiment Result**
Q399R	No Rescue
CYNPSANS(281-290) to RYVPTAGKLT, Q399R	No Rescue
CYNPSANS(281-290) to RYVPTAGKLT, Q399R, R396N	No Rescue
CYNPSANS(281-290) to RYVPTAGKLT, Q399R, R396N, A301K	No Rescue
CYNPSANS(281-290) to RYVPTAGKLT, Q399R, R396N,A301K, TEKLRETT(349-356) to FEQIQKVQ,	No Rescue
CSDGSGSR(266-273) to EKEEQEKL, Q399R, E324K	No Rescue
CYNPSANS(281-290) to RYVPTAGKLT, A301K, TEKLRETT(349-356) FEQIQKVQ, Q399R, R396N, E324K + CSDGSGSR(266-273)EKEEQEKL [Linker]	No Rescue

Table 1 List of mutations performed in attempts to rescue the SytI knockout phenotype by the Rosenmund lab. Although the sequences of SytI C2B and SytVII C2B are nearly 50% identical, none of these additional mutations could improve the rescue. The largest mutation covers nearly 25% of the total number of residues in the domain.

structurally different from SytI C2B. In order to test this hypothesis, I crystallized the protein and determined its structure to atomic resolution. Upon the realization that the structures of SytI C2B and SytVII C2B were extremely similar, I decided to crystallize a C2A domain of a synaptotagmin.

After thawing the frozen cells, they were passed through a cell disruptor at 10,000 psi 5 times. The lysate was then centrifuged at 19,000x g for 30min at 4°C. The remaining supernatant was then subjected to a protamine sulfate treatment at a concentration of 15mg protamine sulfate for every 100mL lysate for 2 hours at room temperature. Protamine sulfate is a peptide that binds to RNA and DNA and then precipitates. We use it in this procedure to lower the overall amount of RNA and DNA that copurifies with the C2B domain, which is highly contaminated with RNA/DNA, just like other members of the Synaptotagmin family. After 2 hours of protamine sulfate treatment the entire solution was again subjected to centrifugation at 19000x g for 30min at 4°C. The supernatant was then added to a slurry of 1.5mL GS4B gluthathione beads. The beads were allowed to react with the protein for 2 hours at room temperature. Next, the beads are extensively washed with PBS buffer until there is no absorbance at 260nm. This typically takes nearly 3L of PBS for a normal 6 L preparation. After this PBS wash, the beads are washed with 250mL PBS+1% Triton X-100, 250mL PBS+1M NaCl, 250mL PBS, and then 20mL 200mM Tris 400mM NaCl. The

beads were then washed with Benzonase Buffer 2 times before undergoing benzonase treatment (discussed in section 2.1.1) for 2 hours at room temperature. After benzonase treatment the beads were washed with 10mL TCB 3 times before treatment with 5-7 units/mL of thrombin to remove the GST affinity tag from the protein.

After elution from the GS4B beads, the protein was injected over a Superdex 75 Hiload 16/60 column using 50mM NaAcetate pH 6.2, 100mM NaCl, 50mM $CaCl_2$ as the buffer. After the S75 column, the protein was then subjected to ion exchange chromatography (Source S) using 50mM NaAcetate pH 6.2, 50mM $CaCl_2$ as buffer A and 50mM NaAcetate pH 6.2, 1M NaCl, 50mM $CaCl_2$ as buffer B. The protein elutes at nearly 300mM NaCl. After elution from the Source S column, the protein was buffer exchanged to 50mM NaAcetate pH 6.2 50mM NaCl 20mM $CaCl_2$ by repeated cycles of concentration-dilution. Protein was then aliquoted and stored at -80°C.

Constructs containing the cDNA of Synaptotagmin 9 C2A domain were a gift from the Sudhof lab. Expression of the C2A domain was relatively straightforward, when compared to that of the C2B domains. BL21 (DE3) cells were transformed with pGEX-KG-SytIX C2A, plated on ampicillin containing agarose plates, and incubated at 37°C for 16 hours. A single colony was picked from one plate and transferred into a flask containing 70mL LB +ampicillin. The flask was then incubated overnight at 37°C. The next morning, 10mL of the

overnight culture was transferred into a larger flask containing 1L LB broth +ampicillin. This culture was then incubated at 37°C with shaking until the OD_{600} reached 0.5-0.8. At this point, the temperature was lowered to 25°C and 400μM IPTG was added to begin induction of SytIX C2A expression. Expression was allowed to continue for approximately 16 hours, at which point the cultures were removed from the incubator and centrifuged at 4000x g for 30min to pellet the cells. The cell pellets were resuspended in PBS buffer containing sigma inhibitor cocktail and 1% Triton X-100. The cells were then passed through a cell disruptor at 10,000psi 5 times. The resulting lysate was then cleared by centrifugation at 19,000x g for 30min at 4°C. The supernatant was then added to a slurry of 2mL GS4B beads for every 1L of culture grown. The beads-lysate mixture was then incubated for 2 hours at room temperature before it was applied to a gravity flow column. The beads were then sequentially washed with 250mL PBS+1% Triton X-100, 250mL PBS+1M NaCl, and then 250mL PBS alone. The beads were then washed with 3x 10mL thrombin cleavage buffer, and then treated with 5-7 units of thrombin per mL of beads. The thrombin reaction was allowed to proceed for 2 hours at room temperature, after which the protein was eluted from the beads. The protein elutes quite purely from the column, and the only further purification step was to inject the protein over a Superdex 75 16/60 gel filtration column using 25mM HEPES pH7.4 and 100mM KCl as the buffer. The protein elutes in a single peak and is quite pure. The protein was then frozen in

liquid nitrogen and stored at -80°C for approximately 3 years, although the importance of this incubation step to the crystallization of the protein is currently unknown.

3.2.2 Phospholipid Binding Assay

In order to ensure that the SytVII C2B domain was properly folded and purified, I tested whether or not the purified domain exhibited Ca^{2+} dependent phospholipid binding activity. I created liposomes using the extrusion method described in section 2.2.3, except for the lipid composition. For these liposomes, I used an 82:15:3 molar ratio of POPC:DOPS:Dansyl-DPPE. Each sample contained 1μM protein, 0.022mg/mL lipid, and either 1μM Ca^{2+} or 2μM EDTA.

I performed these FRET experiments using the native tryptophan residues of the C2B domain as donors, and Dansyl-DPPE as an acceptor. All measurements were recorded using a PTI fluorimeter with slit widths of 2nm at room temperature. The excitation wavelength was 285nm, and the emission spectrum was recorded from 400-650nm.

3.2.3 Crystallization

3.2.3.1 Crystallization of the C2B Domain of SytVII

SytVIIC2B was concentrated to 40mg/ml in 25mM NaAcetate buffer pH 6.2, 50mM KCl, 20mM $CaCl_2$, and 1mM TCEP using a centrifugal concentrator with a molecular weight cutoff of 5000 Daltons. After concentration, a UV spectrum was recorded to determine protein concentration and ensure that the protein was not contaminated by DNA/RNA. Aliquots of the protein were then frozen at -80.

Sitting drop trays were set up using the Art Robbins Instruments Phoenix crystallization robot using 96-condition, 3 subwell Intelliplates. The Intelliplate layout allows for 3 separate protein concentrations to be equilibrated against a single reservoir solution. Each reservoir of the tray was filled with solution from a 96-condition deep-well block containing commercial screen solutions. Using a program on the Phoenix robot, conditions were set up to create dilutions of protein:solution (by volume) at 1:1, 1:2, and 1:3. Plates were incubated at 20°C and imaged every 24 hours.

As the three drops reach equilibrium with the reservoir solution, the sample drops should decrease in volume due to the loss of water. This gradual decrease in volume and concomitant increase in protein concentration allows the protein to enter a state of aggregation. The goal of crystallography is to create an ordered state of aggregation-a crystal.

Initial hits from screening gave crystals with reservoir conditions of 0.2M Li_2SO_4, 0.1M HEPES pH 7.5, and 25% PEG 3350 at 20mg/ml protein. The pH

was optimized from pH 6-9 in steps of 0.5, and the PEG concentration was varied from 2-29%. Large multiple crystals were grown in conditions of 0.2M Li_2SO_4, 0.1M HEPES pH 6.5, and 25% PEG 3350 (**Figure 18**). These crystals were transferred to solutions containing the reservoir solution plus 15% ethylene glycol as a cryoprotectant. The crystals were then frozen in liquid nitrogen.

Single crystals were obtained by growing crystals in similar conditions at 4°C using the same optimization scheme as used for 20°C. The largest single crystals were obtained using a reservoir solution of 0.2M Li_2SO_4, 0.1M HEPES pH 6.5, 18% PEG 3350, and 15% ethylene glycol (**Figure 19**).

3.2.3.2 Crystallization of the C2A Domain of Synaptotagmin IX

The protein was concentrated to 20mg/mL using a Centriprep centrifugal protein concentrator and then used for crystallization trials. Initial crystals were obtained using the sitting drop method and then later optimized using the hanging drop method. Crystals were obtained under a wide range of pHs and salts. The best crystals formed in 200mM ZnAcetate, 18% PEG 8K, and 100mM HEPES pH6.5 (**Figure 20**). These crystals were sent to the Advanced Photon Source synchrotron, Sector 19-ID, and diffracted to 1.44 Å, the limit of the detector.

3.2.4.1 Data Collection, Model Building, and Refinement for the C2B domain of Synaptotagmin VII

Although the crystals initially obtained were not single (**Figure18**), they diffracted to 1.7 Å using the in-house Rigaku FRE rotating anode x-ray generator. I later optimized these crystals to give large single crystals, but the data used for solving the structure of SytVII C2B was obtained using the initial crystals and focusing a synchrotron x-ray beam on a small section of the crystal. Data collected at the synchrotron diffracted to 1.44 Å, the limit of the detector.

The data set was indexed and integrated using HKL3000(Minor, Cymborowski et al. 2006). A search model for molecular replacement was created using the program CHAINSAW(Potterton, Briggs et al. 2003), which prunes non-conserved atoms from a PDB file of a homologous protein; in this case the SytI C2B was used. MOLREP(Potterton, Briggs et al. 2003) searched translation and rotation functions for phasing solutions, and the solution with the highest score was used as a starting point for multiple rounds of refinement and automated model building using ARP/wARP(Potterton, Briggs et al. 2003). 136 of 138 residues in the final structure were initially modeled by Arp/wARP, with the remaining N and C-termini being modeled into electron density using the program COOT(Emsley and Cowtan 2004).

Further rounds of refinement in the program PHENIX (Adams, Grosse-Kunstleve et al. 2002)included using TLS groups determined using the TLSMD server(Painter and Merritt 2006) and my preliminary model as an input. The TLSMD server looks for groups of residues that may be undergoing concerted

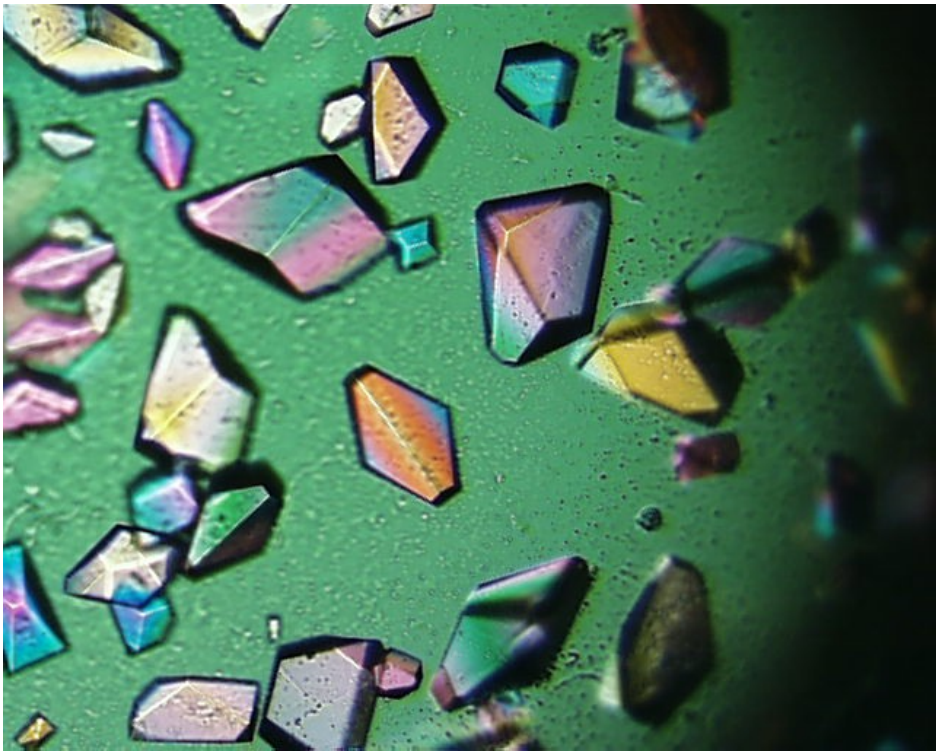

Figure 18. Single crystals of Synaptotagmin 7 C2B domain grown for 3 days at 4° C in 0.2M Li_2SO_4, 0.1M HEPES pH 6.5, 18% PEG 3350, 15% ethylene glycol.

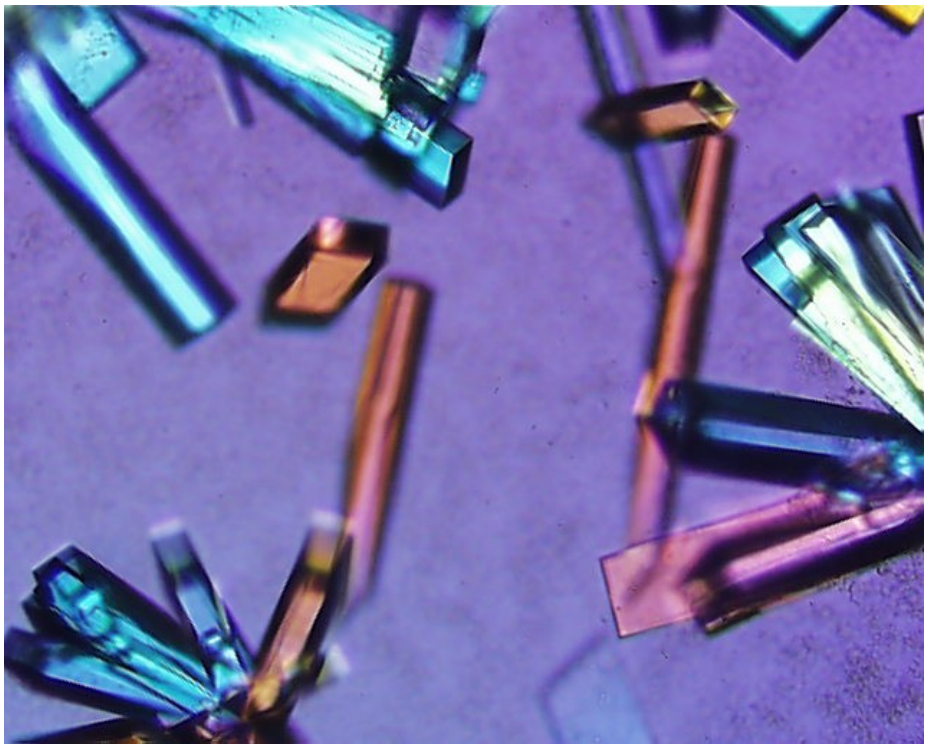

Figure 19. Crystals of SytIX C2A domain. Crystals were grown using the hanging drop method in conditions of 200mM ZnAcetate, 18% PEG 8K, 100mM HEPES pH6.5, and 10% ethylene glycol. Plates were incubated at 20° for approximately 15 minutes. Large single and multiple crystals formed quickly. Only single crystals were sent for synchrotron data collection.

motions. These groups are determined by plotting residue atomic displacement parameters (ADPs, also known colloquially as "B-factors") against residue number. TLS groups have similarly ADPs. The TLSMD output for SytVIIC2B is shown in **Figure 21**.

Refinement was performed using multiple rounds of PHENIX refinement alternated by model re-building in COOT. Through this process, weighting functions were optimized, and anisotropic ADPs were determined. In addition 23 alternate conformations were manually modeled into the experimental electron density. The resulting model was checked using the Molprobity web server (Davis, Leaver-Fay et al. 2007) to ensure adherence to optimal geometry of main and side chains. The final refinement statistics are reported in **Table 2**.

3.2.4.2 Structure Determination and Refinement for the C2A domain of SytIX

The structure of SytIX C2A was solved with MOLREP(Potterton, Briggs et al. 2003) using the structure of Syt1 C2A, modified in the CHAINSAW(Potterton, Briggs et al. 2003) program, as a search model for molecular replacement. A clear solution was obtained, and the model was rebuilt in the program ARP/wARP(Potterton, Briggs et al. 2003). The resulting structure was then refined in the program PHENIX(Adams, Grosse-Kunstleve et al. 2002) followed by alternating cycles of model re-building using the program

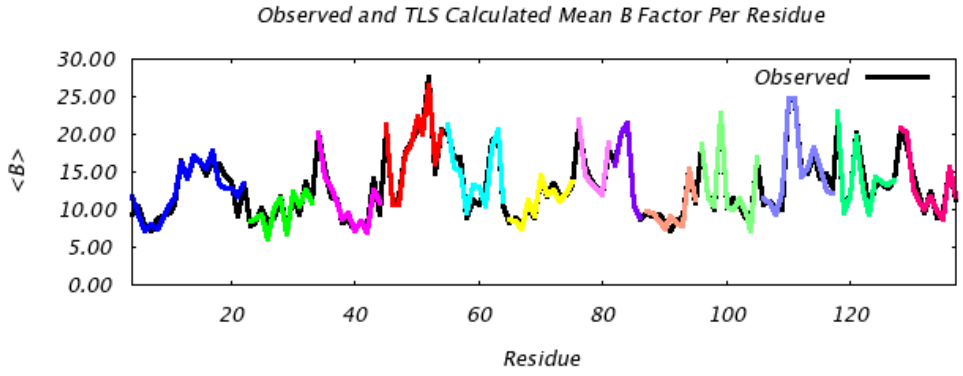

Figure 20 13 TLS groups were calculated for the preliminary model of SytVII C2B domain. These groups were used for TLS refinement in phenix.refine

COOT(Emsley and Cowtan 2004). After a number of iterations, a final model was obtained. The statistics for refinement of the SytIX C2A domain are located in **Table 3**.

3.3 Results and Discussion

Synaptotagmins are multi C2 domain proteins that bind Ca^{2+}/phospholipids to accelerate various regulated secretion processes including neurotransmitter release (SytI/II/IX(Xu, Mashimo et al. 2007)), glucagon exocytosis (SytVII(Gustavsson, Wei et al. 2009)), and a number of other types of secretion (reviewed in (Sudhof 2002)). Individual C2 domains typically have high sequence identity (Sudhof 2002) with each other. Despite this high similarity, Mingshan Xue found that a chimeric synaptotagmin consisting of the SytI C2A domain and the C2B domain of SytVII could not rescue the KO phenotype of SytI KO neurons. This raised the tantalizing possibility that the C2B domain of SytVII was structurally different from the C2B domain of SytI, despite a 48% sequence identity. In order to find out if there indeed were structural changes in SytVII, I crystallized the protein and solved its structure to 1.44Å resolution.

Data Collection	
Space Group	$P2_12_12_1$
Cell Dimensions a, b, c (Å)	35.598, 44.892, 87.383
Wavelength (Å)	1.0148
Resolution Range (Å)	50-1.44 (1.46-1.44)
R_{sym} (%)	3.9 (39.7)
I/σ	31.1 (2.6)
Completeness (%)	98.0 (91.0)
Redundancy	4.7 (4.0)
No. Reflections	25,581 (1,158)
Refinement	
Resolution range (Å)	26.6-1.44 (1.50-1.44)
R_{work} (%)	16.63 (19.56)
R_{free} (%)	19.35 (24.07)
No. Atoms	
Protein/Solvent/Ion	2293 / 161 / 3
Average B-value ($Å^2$)	16.26 / 27.05 / 11.75
RMS deviations	
Bond Lengths (Å)	0.008
Bond Angles (°)	0.953

Table 2 Refinement Statistics for the crystal structure of SytVII C2B

Data Collection	
Space Group	$P2_12_12$
Cell Dimensions a, b, c (Å)	66.827, 67.818, 29.117
Wavelength (Å)	1.0148
Resolution Range (Å)	50-1.44 (1.46-1.44)
R_{sym} (%)	5.5 (31.9)
I/σ	44.5 (4.0)
Completeness (%)	99.5 (94.0)
Redundancy	7.2 (4.8)
No. Reflections	24,625 (1,151)
Refinement	
Resolution range (Å)	22.1-1.44
R_{work} (%)	20.44 (22.78)
R_{free} (%)	24.66(30.19)
No. Atoms	
Protein/Solvent/Ion	2023 / 111 / 4
Average B-value ($Å^2$)	23.5/29.917 /19.775
RMS deviations	
Bond Lengths (Å)	0.010
Bond Angles (°)	1.06

Table 3 Refinement statistics for the crystal structure of the SytIX C2A domain.

The calcium dependent phospholipid binding assay is a fast and sensitive measurement of phospholipid binding. The reliance on native tryptophan residues as FRET donors allows this method to be used without modification of the protein itself. The results of the phospholipid binding test convincingly show that SytVII C2B domain binds phospholipids in the presence of Ca^{2+} (**Figure 21**). Since the protein can perform its function well, it is likely to be well-folded and free of RNA/DNA contamination.

Using this purified protein, large protein crystals were grown using the methods described in section 3.2.3. These crystals diffracted to 1.44Å at the APS beamline and were used to determine the structure of the SytVII C2B domain using molecular replacement. The crystal structure of SytVII C2B domain shows a canonical C2 domain fold. The structure is a beta sandwich of four antiparallel beta sheets each with a single helix bound to the edge of the sandwich (**Figure 22**). The RMS deviation in C_α residues between SytI C2B and SytVII C2B is 0.72Å (**Figure 23**), an extremely close alignment, indicating that there is no

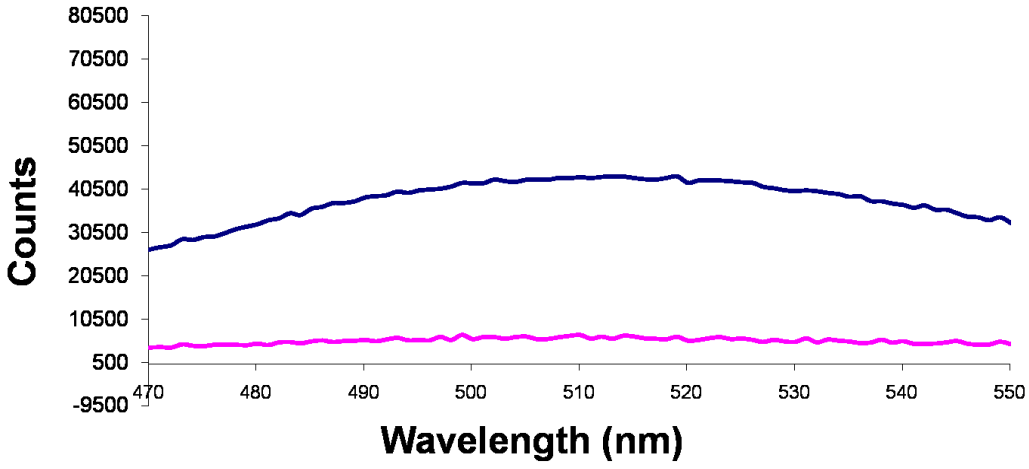
80500
70500
60500
50500
40500
30500
20500
10500
500
-9500
Counts
470
480
490
500
510
520
530
540
550
Wavelength (nm)

Figure 21 Results of the phospholipid binding assay. An intrinsic Trp residue transfers its energy to a Dansyl-labeled lipid on a liposome when the protein is in close proximity to the liposome. Spectra were recorded either with the addition of 1mM Ca^{2+} (**Blue**) or with the addition of 5mM EDTA (**Magenta**). FRET only takes place in the presence of Ca^{2+}, indicating calcium depended phospholipid binding.

Figure 22 A cartoon diagram of the SytVII C2B domain with protein residues colored green and the three bound calcium ions colored brown. The protein forms a beta sandwich with the HA helix contacting the edges of both beta sheets. Figure was prepared using PyMol(W.L. 2002).

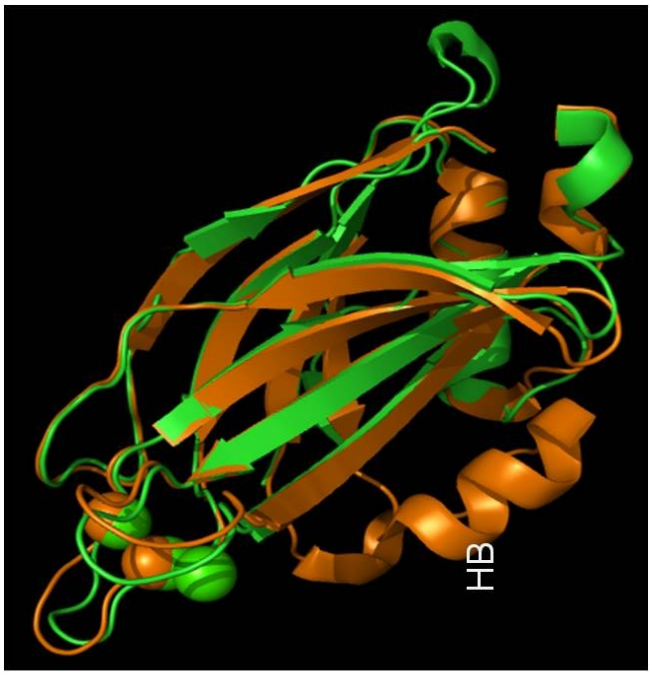
HB


N
C

Figure 23 Overlay of SytVII C2B (green) and SytI C2B (brown). The picture on the right is rotated 180 degrees from the picture on the left. The RMSD of the Cα residues is 0.72Å. The N and C-termini are labeled, as well as the HB helix of SytI C2B. The main differences between the two structures are in the calcium binding loops, where SytVII C2B binds 3 calcium ions instead of 2, and the loss of the HB helix from SytI.

global change in folding. Despite this overall similarity, there are a number of striking differences between the structures of SytI C2B and SytVII C2B.

Comparing the structures of SytI C2B and SytVII C2B yield a number of important observations for the overall function of SytVII. In SytVII C2B, the HB helix is missing from the sequence as well as the structure, and may play a role in the failure of SytI/7 chimeras to rescue the SytI knockout. The calcium binding loops bind 3 calcium ions instead of the 2 found in SytI C2B. This third calcium binding site arises from the introduction of serine 362 to the rest of the conserved calcium binding sites (**Figure 24**). In addition to S362, the coordination of the second calcium binding site is different from the published crystal structure of the SytI C2B domain (Cheng, Sequeira et al. 2004). The findings here instead agree with the solution NMR structure solved in 2001 in our laboratory(Fernandez, Arac et al. 2001). The backbone of residue D371 in the crystal structure of the SytI C2B domain is shifted away from the calcium ion due to crystal packing, and only helps to coordinate the second calcium ion through a hydrogen bond between a side chain carbonyl and an intervening water molecule (**Figure 25**). In the structure of the SytVII C2B domain, this crystal packing interaction is absent, and the side chain carbonyls of the corresponding residue D365 directly coordinate both Ca^{2+} ions 2 and 3. This directly contradicts the claim in (Cheng, Sequeira et al. 2004) that only a longer glutamine side chain in this position could

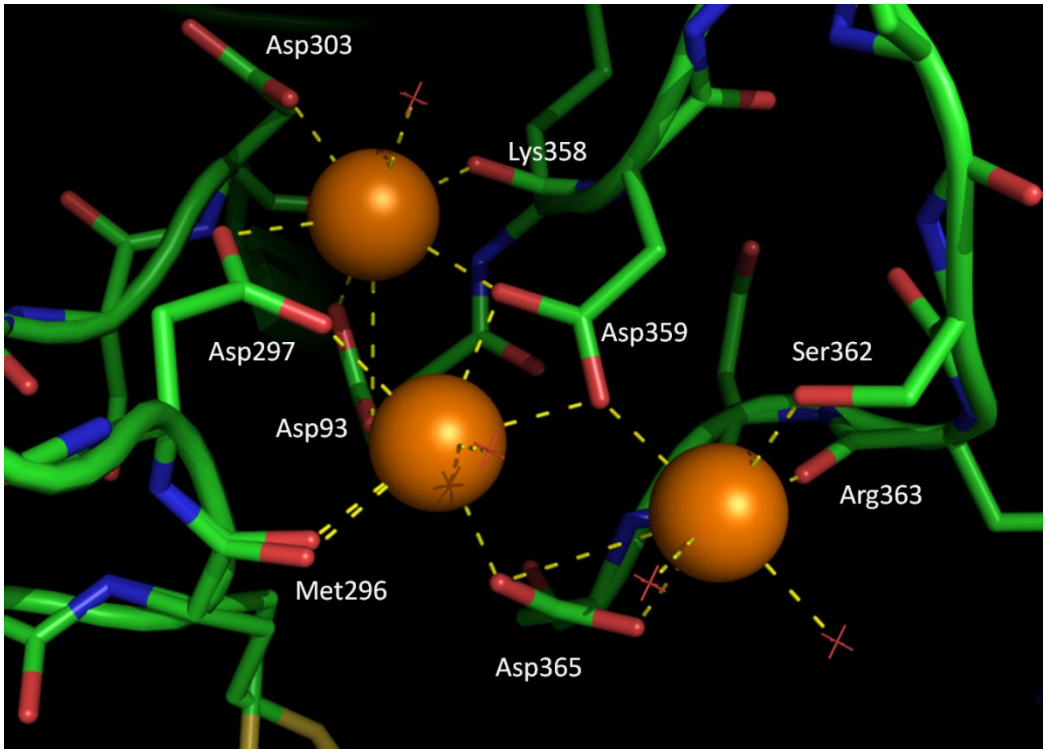

Figure 24 The calcium ion coordinating residues of SytVII C2B. Protein residues are displayed in green with nitrogen atoms as blue and oxygen atoms as red. The addition of Ser362 provides coordination for the third calcium ion that is not present in the structure of SytI C2B. The distance between each of the Ca^{2+} ions is >4Å

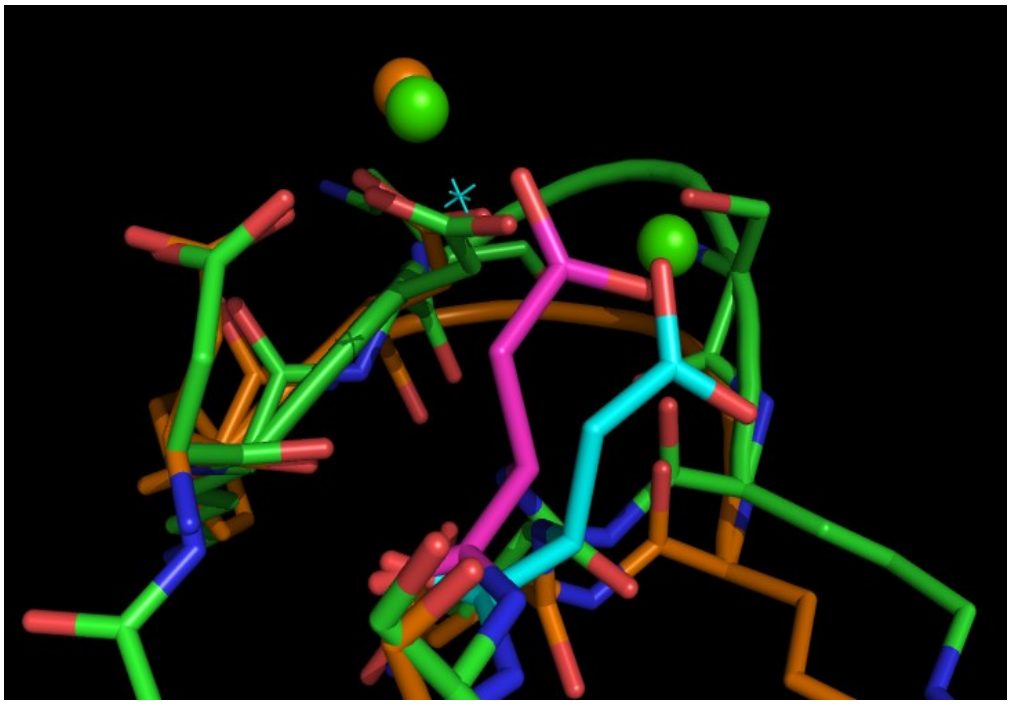

Figure 25 A comparison of the conformation of residue D371 of SytI (Cyan) and D365 of SytVII (Magenta). The crystal structure of SytI C2B domain with calcium bound from (Cheng, Sequeira et al. 2004) is colored in Orange and overlaid with the structure of the SytVII C2B (Green). The calcium ions belonging to each structure are colored similarly to the rest of the domain. There is a clear difference in both the backbone and rotamer conformation of residues D371 and D365. The D371 residue in the SytI C2B crystal structure is deformed by a crystal packing artifact, but still helps to coordinate a water molecule represented as a cyan nonbonded atom. In the SytVII C2B structure residue D365 directly coordinates two Ca^{2+} ions.

directly coordinate a calcium ion. In addition this demonstrates the potential danger that crystal packing artifacts pose when interpreting the structures of proteins. Although this structure solves the question of D371 in SytI C2B, a number of important *in vivo* findings remain unexplained by the structure of SytVII.

Before crystallization trials began, In vivo data from Christian Rosenmund's laboratory showed that a chimera of SytI C2A and SytVII C2B could not rescue function in SytI KO neurons (Rosenmund et al, unpublished data). This result was puzzling because of the high sequence identity between SytI C2B and SytVII C2B, so a number of mutations were designed (**Table 3**). The goal of these mutagenesis experiments was to mutate residues in SytVII C2B to corresponding residues normally found in SytI C2B. Surprisingly, these mutations, the most extensive of which covered an additional 25% of the total sequence of SytVII C2B, could not rescue function of the SytI KO. Although SytVII C2B is highly similar in sequence to SytI C2B, there is a missing c-terminal HB helix that SytI C2B has and SytVII C2B does not. Unpublished results from Rosenmund suggest that this HB helix functions in an inhibitory manner and is likely not the cause of the apparent incompatibility of SytVII C2B and SytI C2B. Upon removal of the HB helix, they report an increase in neurotransmitter release, which does not explain the inhibition of release in the

SytI/VII chimera. So, the question remains as to why the Syt 1/7 chimera does not rescue the SytI KO phenotype.

Ruling out a role of the HB helix leaves the possibility that either there is a C2B related protein-protein interaction that is disrupted by the remaining 25% of the sequence, or the possibility that the chimeric construct is not being properly trafficked to the vesicle surface and is instead perhaps trafficked to a location in the synapse that is incompatible with the normal function of SytI C2B. These possibilities are currently being investigated. One possible way to potentially avoid this problem would be to instead use SytI and then mutate residues on the C2B domain to their corresponding residues on SytVII. This could help to avoid problems with signal sequences that may have been interfered with during the creation of the chimeric SytI/VII protein. In addition I feel that it may be fruitful to investigate the binding affinity of SytVII and the SNARE complex to see if perhaps small changes in the structure of the SNARE binding site could have large implications for the slower type of regulated secretion that SytVII regulates. Regardless of the possible technical difficulties involved in protein engineering projects like the SytI/VII chimera, it is surprising exactly how similar SytI C2B and SytVII C2B are despite having 50% different residues. A number of positions in SytI/VII show side chains that adopt similar conformations, even though they are different residues (**Figure 26**). These similarities led me to crystallize and solve the structure of the C2A domain of SytIX in order to

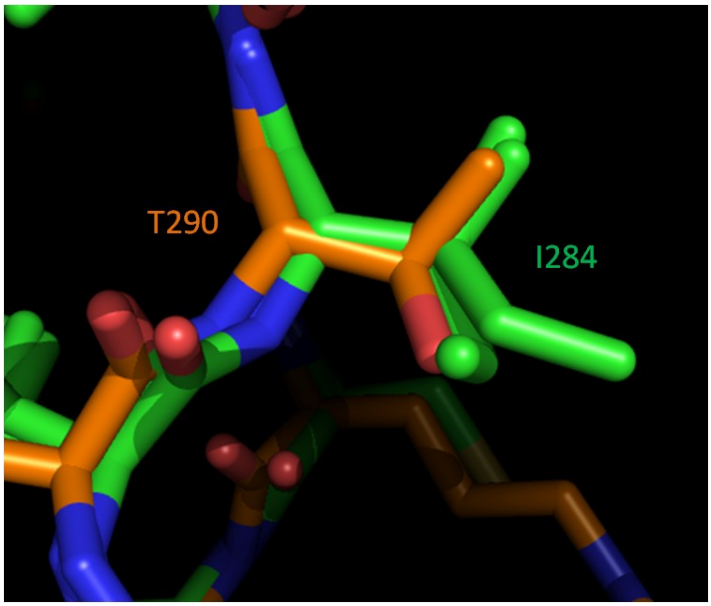
T290
I284

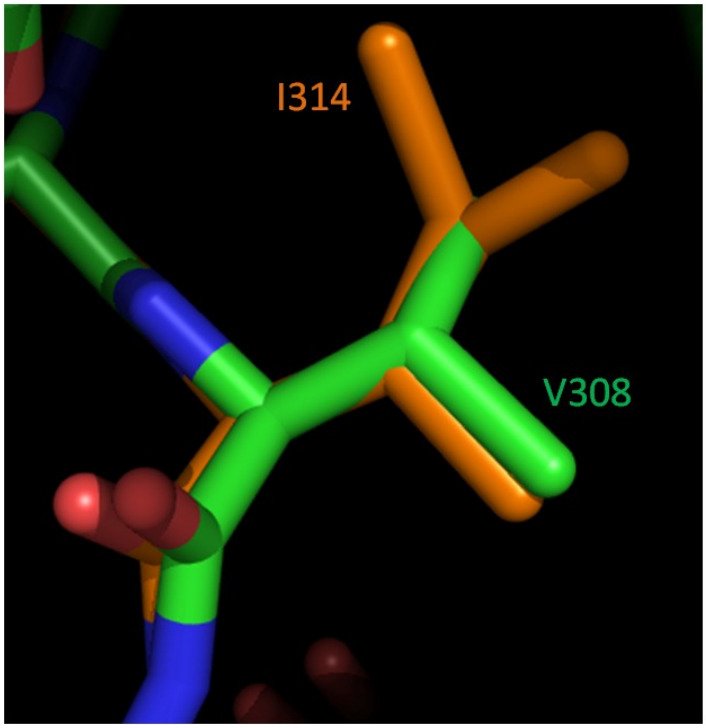
I314
V308

Figure 26 Residues in different C2 domains have surprising similarities even in residues that are different. The structure of SytI C2B (**Orange**) is overlaid with the structure of SytVII C2B (**Green**). Top: the side chains of residues T290 and I284 on SytI C2B and SytVII C2B, respectively, overlap despite the different character of the side chains. Bottom: residues I314 and V308 also show similar side chain rotamers. In both locations the side chains exhibit 1 alternate conformation.

compare it to the C2A domain of SytI and discover just how much variability in protein structure there is between functionally overlapping synaptotagmins. Since both of these proteins are Ca^{2+} sensors for fast neurotransmitter release (Xu, Mashimo et al. 2007), I expected the structures to be very similar.

The structure of the C2A domain of SytIX reveals a structure very similar to the C2A domain of SytI, as expected. The structure is an all beta sandwich with four antiparallel β sheets on each side (**Figure 27**). This crystal structure does had trace calcium in the crystallization condition, and as a result shows two calcium ions bound by the Ca^{2+} binding loops. The overall RMSD deviation of C_α atoms is 0.862Å, which means that the two structures are actually slightly less well aligned than SytI C2B and SytVII C2B. The overlaid structures are shown in **Figure 28**.

Although there is no large difference between the two structures, the structure of the C2A domain of SytIX will be useful in further studies because it will allow electrophysiologists and biochemists to create more informed mutations. The most logical progression of this work would be to determine the Ca^{2+} unbound structure of the SytIX C2A domain and compare it to the Ca^{2+} unbound forms of other synaptotagmin isoforms.

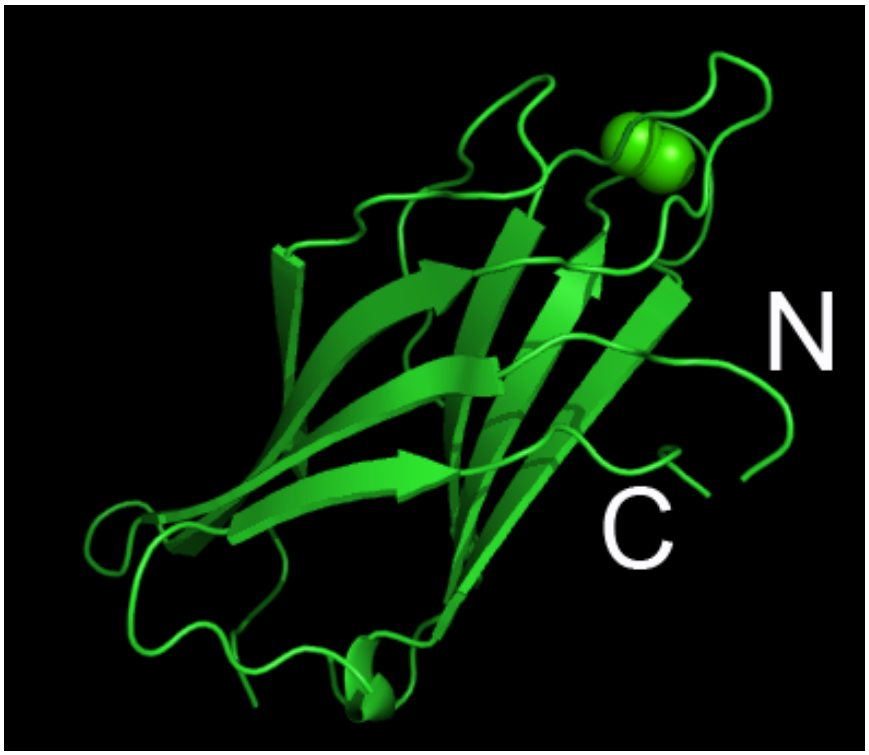

Figure 27 The Crystal structure of the SytIX C2A domain. The C2A domain is an all β-sheet protein with a β-sandwich fold reminiscent of other C2A domains of known structure. The N and C-termini are labeled with the letters "N" and "C" respectively. The image on the left is rotated 180° to make the image on the right.

Figure 28 Aligned structures of SytI C2A (**Orange**) and Syt9 C2A (**Green**) reveal very similar structures. The RMSD for this alignment is 0.862Å, indicating that the two structures are near-super imposable. This result is unsurprising, since SytI,II, and IX are the synaptotagmins that control fast neurotransmitter release.

CHAPTER 4

FUTURE RESEARCH IN NEUROTRANSMITTER RELEASE

The field of membrane fusion and more specifically neurotransmitter release has been extremely active since Hodgkin and Huxley made their first recordings from squid giant axon in 1952(Hodgkin and Huxley 1952). A current search on PebMed for the term "Neurotransmitter release" yields nearly 89,000 research reports, indicating that a large number of groups have been working to understand the incredibly interesting and physiologically important problems of neurotransmission. Since I am interested in the structural biology of release, I am most interested in the structures of various components of the release machinery, and how they all interact in concert to overcome the large energy barrier of membrane fusion. I believe that obtaining these structures will require a number of emerging technologies, such as nanodiscs, as well as some well established ones such as NMR.

Critical to any structural study of membrane fusion proteins, the membrane needs to be present. Although this makes certain types of experiments such as typical x-ray crystallography and NMR difficult, the importance of lipids and membranes in membrane fusion should not be discounted for the sake of

expediency. Including membranes in any experiment introduces a number of additional factors that need to be dealt with, including buffer conditions, homogeneity of lipid-reconstituted complexes, and the tumbling rate of the target reconstituted protein complex. The Rizo laboratory has recently been experimenting with creating nanodiscs. These relatively small particles consist of a small piece of lipid bilayer where the hydrophobic tails of the lipid molecules are protected from the polar solvent by a ring of apolipoprotein A1 (**Figure 29**), and has already been shown to be a good model membrane for reconstituting membrane proteins and studying them by NMR (Civjan, Bayburt et al. 2003; Kijac, Li et al. 2007; Gluck, Wittlich et al. 2009).

Since the Rizo lab has a strong background in NMR, I believe that methods combining selective isotopic labeling of methyls, paramagnetic labeling, nanodisc technology, and transverse relaxation optimized pulse sequences will be a fruitful path to structures on membranes. Indeed, initial experiments using these advanced methods have already begun in our laboratory. Selective methyl labeling takes advantage of the small linewidths and high intensities of methyl signals in highly deuterated environments to produce spectra of remarkable quality, even for very large complexes (Kreishman-Deitrick, Egile et al. 2003). Paramagnetic broadening has been used to help determine protein structures by NMR (reviewed in (Arora and Tamm 2001)). Paramagnetic probes can provide

distance restraints by virtue of their distance dependent broadening of resonances. These distance restraints could then be used for NMR structure calculations.

With the advent of nanodisc techniques for studying protein structure and interactions on the membrane, the structural studies of a number of highly important membrane complexes becomes possible. SNARE complexes with Syt or complexin bound as well as Munc18 and possibly Munc13 would be extremely high value complexes that I believe the Rizo lab should attempt to obtain in order to understand the structural basis for neurotransmitter release. With the current levels of expertise, hard work, and technology, presently in the laboratory, I feel that obtaining these structures is only a matter of time.

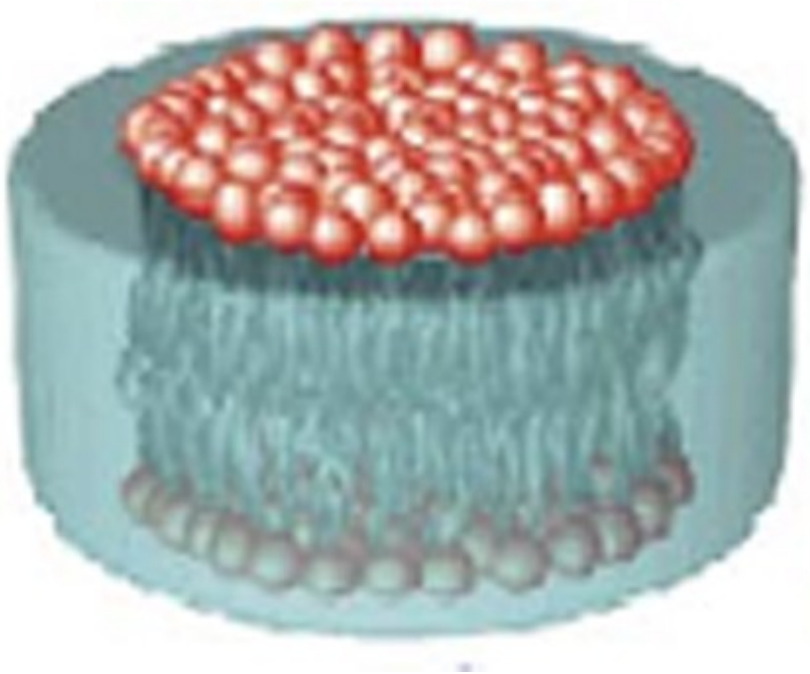

Figure 29 A cartoon representation of a nanodisc. The lipid head groups are exposed to the bulk solvent, while the hydrophobic tails of the lipids are surrounded by a ring of proteins. Engineering of these proteins could possibly produce larger or smaller nanodiscs for a variety of structural biological techniques. This depiction of a nanodisc was adapted from (Civjan, Bayburt et al. 2003)

References

ADAMS, P. D., R. W. GROSSE-KUNSTLEVE, ET AL. (2002). "PHENIX: BUILDING NEW SOFTWARE FOR AUTOMATED CRYSTALLOGRAPHIC STRUCTURE DETERMINATION." ACTA CRYSTALLOGR D BIOL CRYSTALLOGR **58**(PT 11): 1948-54.

ARAC, D., X. CHEN, ET AL. (2006). "CLOSE MEMBRANE-MEMBRANE PROXIMITY INDUCED BY CA(2+)-DEPENDENT MULTIVALENT BINDING OF SYNAPTOTAGMIN-1 TO PHOSPHOLIPIDS." NAT STRUCT MOL BIOL **13**(3): 209-17.

ARORA, A. AND L. K. TAMM (2001). "BIOPHYSICAL APPROACHES TO MEMBRANE PROTEIN STRUCTURE DETERMINATION." CURR OPIN STRUCT BIOL **11**(5): 540-7.

AUGUSTINE, G. J., M. E. BURNS, ET AL. (1996). "EXOCYTOSIS: PROTEINS AND PERTURBATIONS." ANNU REV PHARMACOL TOXICOL **36**: 659-701.

BENNETT, M. K. AND R. H. SCHELLER (1993). "THE MOLECULAR MACHINERY FOR SECRETION IS CONSERVED FROM YEAST TO NEURONS." PROC NATL ACAD SCI U S A **90**(7): 2559-63.

BLASI, J., E. R. CHAPMAN, ET AL. (1993). "BOTULINUM NEUROTOXIN A SELECTIVELY CLEAVES THE SYNAPTIC PROTEIN SNAP-25." NATURE **365**(6442): 160-3.

BLASI, J., E. R. CHAPMAN, ET AL. (1993). "BOTULINUM NEUROTOXIN C1 BLOCKS NEUROTRANSMITTER RELEASE BY MEANS OF CLEAVING HPC-1/SYNTAXIN." EMBO J **12**(12): 4821-8.

BOWEN, M. E., K. WENINGER, ET AL. (2005). "SINGLE-MOLECULE STUDIES OF SYNAPTOTAGMIN AND COMPLEXIN BINDING TO THE SNARE COMPLEX." BIOPHYS J **89**(1): 690-702.

CHAPMAN, E. R., S. AN, ET AL. (1994). "SNAP-25, A T-SNARE WHICH BINDS TO BOTH SYNTAXIN AND SYNAPTOBREVIN VIA DOMAINS THAT MAY FORM COILED COILS." J. BIOL. CHEM. **269**(44): 27427-27432.

CHEN, X. (2002). "THREE-DIMENSIONAL STRUCTURE OF THE COMPLEXIN/SNARE COMPLEX." NEURON **33**: 397-409.

CHEN, X., D. ARAC, ET AL. (2006). "SNARE-MEDIATED LIPID MIXING DEPENDS ON THE PHYSICAL STATE OF THE VESICLES." BIOPHYS J **90**(6): 2062-74.

CHEN, X., D. R. TOMCHICK, ET AL. (2002). "THREE-DIMENSIONAL STRUCTURE OF THE COMPLEXIN/SNARE COMPLEX." NEURON **33**(3): 397-409.

CHENG, Y., S. M. SEQUEIRA, ET AL. (2004). "CRYSTALLOGRAPHIC IDENTIFICATION OF CA2+ AND SR2+ COORDINATION SITES IN SYNAPTOTAGMIN I C2B DOMAIN." PROTEIN SCI **13**(10): 2665-72.

CHICKA, M. C. AND E. R. CHAPMAN (2009). "CONCURRENT BINDING OF COMPLEXIN AND SYNAPTOTAGMIN TO LIPOSOME-EMBEDDED SNARE COMPLEXES (DAGGER)." BIOCHEMISTRY.

CIVJAN, N. R., T. H. BAYBURT, ET AL. (2003). "DIRECT SOLUBILIZATION OF HETEROLOGOUSLY EXPRESSED MEMBRANE PROTEINS BY INCORPORATION INTO NANOSCALE LIPID BILAYERS." BIOTECHNIQUES **35**(3): 556-60, 562-3.

DAI, H., N. SHEN, ET AL. (2007). "A QUATERNARY SNARE-SYNAPTOTAGMIN-CA2+-PHOSPHOLIPID COMPLEX IN NEUROTRANSMITTER RELEASE." J MOL BIOL **367**(3): 848-63.

DAVIS, I. W., A. LEAVER-FAY, ET AL. (2007). "MOLPROBITY: ALL-ATOM CONTACTS AND STRUCTURE VALIDATION FOR PROTEINS AND NUCLEIC ACIDS." NUCLEIC ACIDS RES **35**(WEB SERVER ISSUE): W375-83.

DULUBOVA, I., M. KHVOTCHEV, ET AL. (2007). "MUNC18-1 BINDS DIRECTLY TO THE NEURONAL SNARE COMPLEX." PROC NATL ACAD SCI U S A **104**(8): 2697-702.

EASTWOOD, S. L., P. W. BURNET, ET AL. (2000). "EXPRESSION OF COMPLEXIN I AND II MRNAS AND THEIR REGULATION BY ANTIPSYCHOTIC DRUGS IN THE RAT FOREBRAIN." SYNAPSE **36**(3): 167-77.

EASTWOOD, S. L. AND P. J. HARRISON (2000). "HIPPOCAMPAL SYNAPTIC PATHOLOGY IN SCHIZOPHRENIA, BIPOLAR DISORDER AND MAJOR DEPRESSION: A STUDY OF COMPLEXIN MRNAS." MOL PSYCHIATRY **5**(4): 425-32.

EDWARDSON, J. M., C. T. WANG, ET AL. (2003). "EXPRESSION OF MUTANT HUNTINGTIN BLOCKS EXOCYTOSIS IN PC12 CELLS BY DEPLETION OF COMPLEXIN II." J BIOL CHEM **278**(33): 30849-53.

EMSLEY, P. AND K. COWTAN (2004). "COOT: MODEL-BUILDING TOOLS FOR MOLECULAR GRAPHICS." ACTA CRYSTALLOGR D BIOL CRYSTALLOGR **60**(PT 12 PT 1): 2126-32.

FERNANDEZ-CHACON, R. (2001). "SYNAPTOTAGMIN I FUNCTIONS AS A CALCIUM REGULATOR OF RELEASE PROBABILITY." NATURE **410**: 41-49.

FERNANDEZ-CHACON, R., O. H. SHIN, ET AL. (2002). "STRUCTURE/FUNCTION ANALYSIS OF CA2+ BINDING TO THE C2A DOMAIN OF SYNAPTOTAGMIN 1." J NEUROSCI **22**(19): 8438-46.

FERNANDEZ, I., D. ARAC, ET AL. (2001). "THREE-DIMENSIONAL STRUCTURE OF THE SYNAPTOTAGMIN 1 C2B-DOMAIN: SYNAPTOTAGMIN 1 AS A PHOSPHOLIPID BINDING MACHINE." NEURON **32**(6): 1057-1069.

FERNANDEZ, I., J. UBACH, ET AL. (1998). "THREE-DIMENSIONAL STRUCTURE OF AN EVOLUTIONARILY CONSERVED N-TERMINAL DOMAIN OF SYNTAXIN 1A." CELL **94**(6): 841-9.

FERRO-NOVICK, S. AND R. JAHN (1994). "VESICLE FUSION FROM YEAST TO MAN." NATURE **370**(6486): 191-3.

FESCE, R., F. GROHOVAZ, ET AL. (1994). "NEUROTRANSMITTER RELEASE: FUSION OR 'KISS-AND-RUN'?" TRENDS CELL BIOL **4**(1): 1-4.

GEPPERT, M. AND T. C. SUDHOF (1998). "RAB3 AND SYNAPTOTAGMIN: THE YIN AND YANG OF SYNAPTIC MEMBRANE FUSION." ANNU REV NEUROSCI **21**: 75-95.

GERASIMENKO, J. V., O. V. GERASIMENKO, ET AL. (2001). "MEMBRANE REPAIR: CA(2+)-ELICITED LYSOSOMAL EXOCYTOSIS." CURR BIOL **11**(23): R971-4.

GIRAUDO, C. G., A. GARCIA-DIAZ, ET AL. (2009). "ALTERNATIVE ZIPPERING AS AN ON-OFF SWITCH FOR SNARE-MEDIATED FUSION." SCIENCE **323**(5913): 512-6.

GIRAUDO, C. G., A. GARCIA-DIAZ, ET AL. (2008). "DISTINCT DOMAINS OF COMPLEXINS BIND SNARE COMPLEXES AND CLAMP FUSION IN VITRO." J BIOL CHEM **283**(30): 21211-9.

GLUCK, J. M., M. WITTLICH, ET AL. (2009). "INTEGRAL MEMBRANE PROTEINS IN NANODISCS CAN BE STUDIED BY SOLUTION NMR SPECTROSCOPY." J AM CHEM SOC.

GRAY, E. G. (1959). "ELECTRON MICROSCOPY OF SYNAPTIC CONTACTS ON DENDRITE SPINES OF THE CEREBRAL CORTEX." NATURE **183**(4675): 1592-3.

GRISE, F., N. TAIB, ET AL. (2007). "DISTINCT ROLES OF THE C2A AND THE C2B DOMAIN OF THE VESICULAR CA2+ SENSOR SYNAPTOTAGMIN 9 IN ENDOCRINE BETA-CELLS." BIOCHEM J **403**(3): 483-92.

GUSTAVSSON, N., S. H. WEI, ET AL. (2009). "SYNAPTOTAGMIN-7 IS A PRINCIPAL CA2+ SENSOR FOR CA2+ -INDUCED GLUCAGON EXOCYTOSIS IN PANCREAS." J PHYSIOL **587**(PT 6): 1169-78.

HAYASHI, T., S. YAMASAKI, ET AL. (1995). "DISASSEMBLY OF THE RECONSTITUTED SYNAPTIC VESICLE MEMBRANE FUSION COMPLEX IN VITRO." EMBO J **14**(10): 2317-25.

HESS, D. T., T. M. SLATER, ET AL. (1992). "THE 25 KDA SYNAPTOSOMAL-ASSOCIATED PROTEIN SNAP-25 IS THE MAJOR METHIONINE-RICH POLYPEPTIDE IN RAPID AXONAL TRANSPORT AND A MAJOR SUBSTRATE FOR PALMITOYLATION IN ADULT CNS." J NEUROSCI **12**(12): 4634-41.

HODGKIN, A. L. AND A. F. HUXLEY (1952). "A QUANTITATIVE DESCRIPTION OF MEMBRANE CURRENT AND ITS APPLICATION TO CONDUCTION AND EXCITATION IN NERVE." J PHYSIOL **117**(4): 500-44.

JAHN, R. AND T. C. SUDHOF (1999). "MEMBRANE FUSION AND EXOCYTOSIS." ANNU REV BIOCHEM **68**: 863-911.

KIJAC, A. Z., Y. LI, ET AL. (2007). "MAGIC-ANGLE SPINNING SOLID-STATE NMR SPECTROSCOPY OF NANODISC-EMBEDDED HUMAN CYP3A4." BIOCHEMISTRY **46**(48): 13696-703.

KREISHMAN-DEITRICK, M., C. EGILE, ET AL. (2003). "NMR ANALYSIS OF METHYL GROUPS AT 100-500 KDA: MODEL SYSTEMS AND ARP2/3 COMPLEX." BIOCHEMISTRY **42**(28): 8579-86.

LAKOWICZ, J. R. (2006). PRINCIPLES OF FLUORESCENCE SPECTROSCOPY. NEW YORK, SPRINGER.

LI, Y., G. J. AUGUSTINE, ET AL. (2007). "KINETICS OF COMPLEXIN BINDING TO THE SNARE COMPLEX: CORRECTING SINGLE MOLECULE FRET MEASUREMENTS FOR HIDDEN EVENTS." BIOPHYS J **93**(6): 2178-87.

LIN, R. C. AND R. H. SCHELLER (1997). "STRUCTURAL ORGANIZATION OF THE SYNAPTIC EXOCYTOSIS CORE COMPLEX." NEURON **19**: 1087-1094.

LINK, E., L. EDELMANN, ET AL. (1992). "TETANUS TOXIN ACTION: INHIBITION OF NEUROTRANSMITTER RELEASE LINKED TO SYNAPTOBREVIN PROTEOLYSIS." BIOCHEM BIOPHYS RES COMMUN **189**(2): 1017-23.

LINK, E., H. MCMAHON, ET AL. (1993). "CLEAVAGE OF CELLUBREVIN BY TETANUS TOXIN DOES NOT AFFECT FUSION OF EARLY ENDOSOMES." J BIOL CHEM **268**(25): 18423-6.

LITTLETON, J. T., M. STERN, ET AL. (1993). "MUTATIONAL ANALYSIS OF DROSOPHILA SYNAPTOTAGMIN DEMONSTRATES ITS ESSENTIAL ROLE IN CA(2+)-ACTIVATED NEUROTRANSMITTER RELEASE." CELL **74**(6): 1125-34.

LIU, J., T. GUO, ET AL. (2006). "COMPLEXIN IS ABLE TO BIND TO SNARE CORE COMPLEXES IN DIFFERENT ASSEMBLED STATES WITH DISTINCT AFFINITY." BIOCHEM BIOPHYS RES COMMUN **347**(2): 413-9.

LIU, J., T. GUO, ET AL. (2007). "OVEREXPRESSION OF COMPLEXIN IN PC12 CELLS INHIBITS EXOCYTOSIS BY PREVENTING SNARE COMPLEX RECYCLING." BIOCHEMISTRY (MOSC) **72**(4): 439-44.

MARTINEZ, I., S. CHAKRABARTI, ET AL. (2000). "SYNAPTOTAGMIN VII REGULATES CA(2+)-DEPENDENT EXOCYTOSIS OF LYSOSOMES IN FIBROBLASTS." J CELL BIOL **148**(6): 1141-49.

MAXIMOV, A., Y. LAO, ET AL. (2008). "GENETIC ANALYSIS OF SYNAPTOTAGMIN-7 FUNCTION IN SYNAPTIC VESICLE EXOCYTOSIS." PROC NATL ACAD SCI U S A **105**(10): 3986-91.

MAXIMOV, A., J. TANG, ET AL. (2009). "COMPLEXIN CONTROLS THE FORCE TRANSFER FROM SNARE COMPLEXES TO MEMBRANES IN FUSION." SCIENCE **323**(5913): 516-21.

MCGUFFIN, L. J., K. BRYSON, ET AL. (2000). "THE PSIPRED PROTEIN STRUCTURE PREDICTION SERVER." BIOINFORMATICS **16**(4): 404-5.

MCMAHON, H. T., M. MISSLER, ET AL. (1995). "COMPLEXINS: CYTOSOLIC PROTEINS THAT REGULATE SNAP RECEPTOR FUNCTION." CELL **83**(1): 111-9.

MINOR, W., M. CYMBOROWSKI, ET AL. (2006). "HKL-3000: THE INTEGRATION OF DATA REDUCTION AND STRUCTURE SOLUTION--FROM DIFFRACTION IMAGES TO AN INITIAL MODEL IN MINUTES." ACTA CRYSTALLOGR D BIOL CRYSTALLOGR **62**(PT 8): 859-66.

MISURA, K. M., R. H. SCHELLER, ET AL. (2000). "THREE-DIMENSIONAL STRUCTURE OF THE NEURONAL-SEC1-SYNTAXIN 1A COMPLEX." NATURE **404**(6776): 355-62.

MORTON, A. J. AND J. M. EDWARDSON (2001). "PROGRESSIVE DEPLETION OF COMPLEXIN II IN A TRANSGENIC MOUSE MODEL OF HUNTINGTON'S DISEASE." J NEUROCHEM **76**(1): 166-72.

NONET, M. L., K. GRUNDAHL, ET AL. (1993). "SYNAPTIC FUNCTION IS IMPAIRED BUT NOT ELIMINATED IN C. ELEGANS MUTANTS LACKING SYNAPTOTAGMIN." CELL **73**(7): 1291-305.

O'CONNOR, V. M., O. SHAMOTIENKO, ET AL. (1993). "ON THE STRUCTURE OF THE 'SYNAPTOSECRETOSOME'. EVIDENCE FOR A NEUREXIN/SYNAPTOTAGMIN/SYNTAXIN/CA2+ CHANNEL COMPLEX." FEBS LETT **326**(1-3): 255-60.

PABST, S., J. W. HAZZARD, ET AL. (2000). "SELECTIVE INTERACTION OF COMPLEXIN WITH THE NEURONAL SNARE COMPLEX. DETERMINATION OF THE BINDING REGIONS." J BIOL CHEM **275**(26): 19808-18.

PABST, S., M. MARGITTAI, ET AL. (2002). "RAPID AND SELECTIVE BINDING TO THE SYNAPTIC SNARE COMPLEX SUGGESTS A MODULATORY ROLE OF COMPLEXINS IN NEUROEXOCYTOSIS." J BIOL CHEM **277**(10): 7838-48.

PAINTER, J. AND E. A. MERRITT (2006). "OPTIMAL DESCRIPTION OF A PROTEIN STRUCTURE IN TERMS OF MULTIPLE GROUPS UNDERGOING TLS MOTION." ACTA CRYSTALLOGR D BIOL CRYSTALLOGR **62**(PT 4): 439-50.

PERIN, M. S., V. A. FRIED, ET AL. (1990). "PHOSPHOLIPID BINDING BY A SYNAPTIC VESICLE PROTEIN HOMOLOGOUS TO THE REGULATORY REGION OF PROTEIN KINASE C." NATURE **345**(6272): 260-3.

POTTERTON, E., P. BRIGGS, ET AL. (2003). "A GRAPHICAL USER INTERFACE TO THE CCP4 PROGRAM SUITE." ACTA CRYSTALLOGR D BIOL CRYSTALLOGR **59**(PT 7): 1131-7.

REIM, K. (2001). "COMPLEXINS REGULATE A LATE STEP IN CA2+-DEPENDENT NEUROTRANSMITTER RELEASE." CELL **104**: 71-81.

REIM, K., M. MANSOUR, ET AL. (2001). "COMPLEXINS REGULATE A LATE STEP IN CA2+-DEPENDENT NEUROTRANSMITTER RELEASE." CELL **104**(1): 71-81.

RIZO, J. AND T. C. SUDHOF (2002). "SNARES AND MUNC18 IN SYNAPTIC VESICLE FUSION." NAT REV NEUROSCI **3**(8): 641-53.

ROGGERO, C. M., G. A. DE BLAS, ET AL. (2007). "COMPLEXIN/SYNAPTOTAGMIN INTERPLAY CONTROLS ACROSOMAL EXOCYTOSIS." J BIOL CHEM **282**(36): 26335-43.

SABATINI, B. L. AND W. G. REGEHR (1999). "TIMING OF SYNAPTIC TRANSMISSION." ANNU REV PHYSIOL **61**: 521-42.

SAWADA, K., C. E. YOUNG, ET AL. (2002). "ALTERED IMMUNOREACTIVITY OF COMPLEXIN PROTEIN IN PREFRONTAL CORTEX IN SEVERE MENTAL ILLNESS." MOL PSYCHIATRY **7**(5): 484-92.

SCHIAVO, G., O. ROSSETTO, ET AL. (1992). "BOTULINUM NEUROTOXINS ARE ZINC PROTEINS." J BIOL CHEM **267**(33): 23479-83.

SCHONN, J. S., A. MAXIMOV, ET AL. (2008). "SYNAPTOTAGMIN-1 AND -7 ARE FUNCTIONALLY OVERLAPPING CA2+ SENSORS FOR

EXOCYTOSIS IN ADRENAL CHROMAFFIN CELLS." PROC NATL ACAD SCI U S A **105**(10): 3998-4003.

SEILER, F., J. MALSAM, ET AL. (2009). "A ROLE OF COMPLEXIN-LIPID INTERACTIONS IN MEMBRANE FUSION." FEBS LETT **583**(14): 2343-8.

SHAO, X., I. FERNANDEZ, ET AL. (1998). "SOLUTION STRUCTURES OF THE CA2+-FREE AND CA2+-BOUND C2A DOMAIN OF SYNAPTOTAGMIN I: DOES CA2+ INDUCE A CONFORMATIONAL CHANGE?" BIOCHEMISTRY **37**(46): 16106-15.

SHIN, O. H., A. MAXIMOV, ET AL. (2004). "UNEXPECTED CA2+-BINDING PROPERTIES OF SYNAPTOTAGMIN 9." PROC NATL ACAD SCI U S A **101**(8): 2554-9.

SOLLNER, T., M. K. BENNETT, ET AL. (1993). "A PROTEIN ASSEMBLY-DISASSEMBLY PATHWAY IN VITRO THAT MAY CORRESPOND TO SEQUENTIAL STEPS OF SYNAPTIC VESICLE DOCKING, ACTIVATION, AND FUSION." CELL **75**(3): 409-18.

SOLLNER, T. H. (2003). "REGULATED EXOCYTOSIS AND SNARE FUNCTION (REVIEW)." MOL MEMBR BIOL **20**(3): 209-20.

SUDHOF, T. C. (1995). "THE SYNAPTIC VESICLE CYCLE: A CASCADE OF PROTEIN-PROTEIN INTERACTIONS." NATURE **375**(6533): 645-53.

SUDHOF, T. C. (2002). "SYNAPTOTAGMINS: WHY SO MANY?" J BIOL CHEM **277**(10): 7629-32.

SUDHOF, T. C. (2004). "THE SYNAPTIC VESICLE CYCLE." ANNU REV NEUROSCI **27**: 509-47.

SUDHOF, T. C., P. DE CAMILLI, ET AL. (1993). "MEMBRANE FUSION MACHINERY: INSIGHTS FROM SYNAPTIC PROTEINS." CELL **75**(1): 1-4.

SUGITA, S., W. HAN, ET AL. (2001). "SYNAPTOTAGMIN VII AS A PLASMA MEMBRANE CA(2+) SENSOR IN EXOCYTOSIS." NEURON **30**(2): 459-73.

SUTTON, R. B., B. A. DAVLETOV, ET AL. (1995). "STRUCTURE OF THE FIRST C2 DOMAIN OF SYNAPTOTAGMIN I: A NOVEL CA2+/PHOSPHOLIPID-BINDING FOLD." CELL **80**(6): 929-38.

SUTTON, R. B., D. FASSHAUER, ET AL. (1998). "CRYSTAL STRUCTURE OF A SNARE COMPLEX INVOLVED IN SYNAPTIC EXOCYTOSIS AT 2.4 A RESOLUTION." NATURE **395**: 347-353.

SUTTON, R. B., D. FASSHAUER, ET AL. (1998). "CRYSTAL STRUCTURE OF A SNARE COMPLEX INVOLVED IN SYNAPTIC EXOCYTOSIS AT 2.4 A RESOLUTION." NATURE **395**(6700): 347-53.

TANG, J., A. MAXIMOV, ET AL. (2006). "A COMPLEXIN/SYNAPTOTAGMIN 1 SWITCH CONTROLS FAST SYNAPTIC VESICLE EXOCYTOSIS." CELL **126**(6): 1175-87.

TUCKER, W. C., J. M. EDWARDSON, ET AL. (2003). "IDENTIFICATION OF SYNAPTOTAGMIN EFFECTORS VIA ACUTE INHIBITION OF SECRETION FROM CRACKED PC12 CELLS." J CELL BIOL **162**(2): 199-209.

W.L., D. (2002). THE PYMOL MOLECULAR GRAPHICS SYSTEM, DELANO SCIENTIFIC.

XU, J., T. MASHIMO, ET AL. (2007). "SYNAPTOTAGMIN-1, -2, AND -9: CA(2+) SENSORS FOR FAST RELEASE THAT SPECIFY DISTINCT PRESYNAPTIC PROPERTIES IN SUBSETS OF NEURONS." NEURON **54**(4): 567-81.

XUE, M., K. REIM, ET AL. (2007). "DISTINCT DOMAINS OF COMPLEXIN I DIFFERENTIALLY REGULATE NEUROTRANSMITTER RELEASE." NAT STRUCT MOL BIOL **14**(10): 949-58.

XUE, M., K. REIM, ET AL. (2007). "DISTINCT DOMAINS OF COMPLEXIN I DIFFERENTIALLY REGULATE NEUROTRANSMITTER RELEASE." NAT STRUCT MOL BIOL.

YOON, T. Y., X. LU, ET AL. (2008). "COMPLEXIN AND CA2+ STIMULATE SNARE-MEDIATED MEMBRANE FUSION." NAT STRUCT MOL BIOL **15**(7): 707-13.